Liu *et al. Microstructures* **2025**, *5*, 2025023
DOI: 10.20517/microstructures.2024.62

Microstructures

Review

Open Access

Check for updates

Layered double hydroxides supported noble-metal single-atom catalysts: precise synthesis, microenvironment regulation, and diverse applications

Dawei Liu, Tianyu Zhang, Xiaoju Gu, Xiang Yang, Aijuan Han, Junfeng Liu

State Key Laboratory of Chemical Resource Engineering, Beijing University of Chemical Technology, Beijing 100029, China.

Correspondence to: Prof. Junfeng Liu and Prof. Aijuan Han, State Key Laboratory of Chemical Resource Engineering, Beijing University of Chemical Technology, 15 Beisanhuan East Road, Chaoyang District, Beijing 100029, China. E-mail: ljf@mail.buct.edu.cn; E-mail: hanaijuan@mail.buct.edu.cn

How to cite this article: Liu, D.; Zhang, T.; Gu, X.; Yang, X.; Han, A.; Liu, J. Layered double hydroxides supported noble-metal single-atom catalysts: precise synthesis, microenvironment regulation, and diverse applications. *Microstructures* **2025**, *5*, 2025023. https://dx.doi.org/10.20517/microstructures.2024.62

Received: 25 Jul 2024 **First Decision:** 30 Aug 2024 **Revised:** 12 Sep 2024 **Accepted:** 26 Sep 2024 **Published:** 25 Feb 2025

Academic Editor: Yida Deng **Copy Editor:** Ping Zhang **Production Editor:** Ping Zhang

Abstract

Noble-metal single-atom catalysts (SACs) have arisen as a research hotspot in heterogeneous catalysis resulting from superior noble-metal-atom utilization, well-defined catalytic centers, and tunable microenvironments. Recently, the advent and rise of noble-metal SACs supported by layered double hydroxides (LDHs) have injected fresh vitality and vigor into this research field. LDHs offer distinct advantages as the support of SACs, such as an ordered and adjustable crystal structure, a two-dimensional layered structure possessing a large specific surface area, facile synthesis with cost-effectiveness, and strong co-catalytic metal-support interaction between LDHs and noble-metal single atoms. In this review, we classified and comprehensively outlined the current synthesis strategies of noble-metal SACs supported by LDHs, and conducted an in-depth analysis of the specific mechanisms underlying each strategy. Subsequently, considering the critical role of the microenvironment of SACs in affecting their catalytic-related properties, we discussed the current microenvironment regulation strategies of LDH-supported noble-metal SACs. We also provide an introduction to the characterization techniques for noble-metal singe-atom sites in LDH-supported noble-metal SACs. Furthermore, we outlined the diverse applications of LDH-supported noble-metal SACs in various catalytic fields and discussed the roles played by noble-metal atoms and LDHs in relevant catalytic processes. Finally, we delineated the challenges and future research directions for the development of LDH-supported noble-metal SACs.

Keywords: Single-atom catalysts, layered double hydroxides, noble-metal atoms, composites, synthesis strategies, applications

INTRODUCTION

Catalysis is pivotal to the modern chemical industry, with noble metals being highly esteemed for their exceptional catalytic activity[1-9]. However, the suboptimal utilization efficiency of noble-metal atoms and the ambiguous composition of catalytic centers present formidable challenges[10,11]. The advent of single-atom catalysts (SACs) offers an enticing solution to augment atom utilization and establish precise identification of active sites. First presented by Qiao *et al.* in 2011, the concept of single-atom catalysis has swiftly garnered significant attention, establishing itself as an emerging research field in catalysis[12-18]. SACs represent a unique class of catalysts, where the active metal atoms are coordinated with atoms from the supports and dispersed as isolated entities on the supports, effectively bridging the gap between heterogeneous and homogeneous catalysis[19-23]. They possess advantages including well-defined and uniform active sites, 100% theoretical utilization of active sites, and adjustable coordination numbers of metal atoms[24-28]. Consequently, SACs present a significant opportunity to minimize the usage of noble metals and maximize catalytic efficiency through precise control over noble-metal active centers. In recent years, significant achievement has been gained in the advancement of SACs.

Since the noble-metal atoms incline toward aggregating because of the high surface free energy, choosing the proper supports is a crucial prerequisite to achieving efficient noble-metal SACs. The utilization of layered double hydroxides (LDHs) as noble-metal SAC supports has recently attracted widespread attention[29,30]. LDHs are a type of two-dimensional layered material composed of positively charged laminates and negatively charged interlayer anions[31]. The chemical formula of LDHs is $[M_{1-x}^{2+}M_x^{3+}(OH)_2]^{x+}A_{x/n}^{n-}\cdot zH_2O$, where M^{2+}/M^{3+} signifies divalent/trivalent metal ions, A^{n-} represents interlayer anions, and the range of x is between 0.17 and 0.33[32]. LDHs offer distinct advantages as the supports of SACs[33-37]: (1) LDHs possess a well-defined structure based on the lamellar ion repulsion theory, laying a crucial foundation for the precise construction of the single-atom sites with well-defined microenvironments; (2) LDHs have strong structural diversity due to the variability of metal cations and interlayer anions, providing more flexibility in tuning the electronic interactions and anchoring strength between the single-atom sites and supports; (3) the LDHs exhibit a notable combination of high specific surface area and a thin two-dimensional structure, facilitating the loading and exposure of metal single-atom sites, thereby enhancing reaction efficiency and maximizing the utilization of active sites; (4) LDHs are characterized by their facile synthesis, cost-effectiveness, and environmental compatibility, making them ideal for large-scale industrial production. While the applications of LDH-supported noble-metal SACs have been extensively researched, a comprehensive summary of current research findings and guidance for future research avenues is still lacking.

In this review, we first comprehensively outline the reported synthetic strategies of LDH-supported noble-metal SACs based on their fundamental preparation principles, including co-precipitation strategy, impregnation strategy, and ion exchange strategy [Figure 1], and discuss the specific mechanisms and various synthesis steps of each strategy. Subsequently, we discuss microenvironment regulation strategies for LDH-supported noble-metal SACs, involving defect engineering strategy and axial coordination engineering strategy. Additionally, we introduce the characterization techniques for noble-metal singe-atom sites in LDH-supported noble-metal SACs, including X-ray absorption spectroscopy (XAS), aberration-corrected high-angle annular dark-field scanning transmission electron microscopy (AC HAADF-STEM), and density functional theory (DFT) calculation. Furthermore, we provide an overview of the current applications of LDH-supported noble-metal SACs in the catalysis field, such as electrocatalysis, thermal catalysis, photocatalysis, and enzyme-like catalysis, and discuss the theoretical and

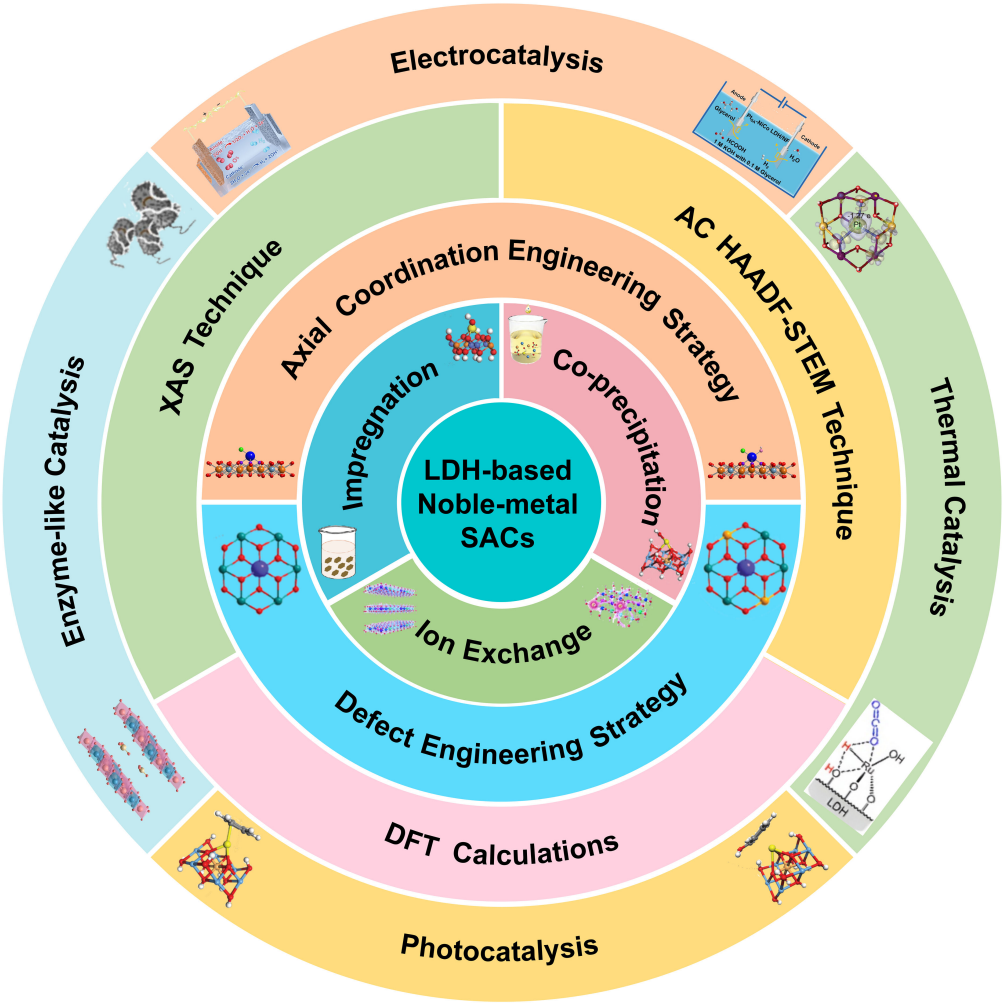

Figure 1. A summary of the key themes in this review. XAS: X-ray absorption spectroscopy; DFT: Density functional theory; AC HAADF-STEM: Aberration-corrected high-angle annular dark-field scanning transmission electron microscopy; LDH: Layered double hydroxides; SACs: Single-atom catalysts.

experimental evidence supporting their catalytic mechanisms. Finally, we address the existing limitations and future opportunities and challenges associated with LDH-supported noble-metal SACs, including the precise turning of noble-metal single-atom sites, the high loading of noble-metal single-atom sites, the role of interlayer anions in LDHs, the stability of LDH-supported noble-metal SACs, the development of dual/multiple atom catalysts (DACs/MACs), the application of in-situ characterization, the establishment of advanced intelligent synthesis platforms, further exploration in application fields, and large-scale industrial production.

THE SYNTHESIS STRATEGIES OF LDH-SUPPORTED NOBLE-METAL SACS

Due to the distinctive structural characteristics of LDHs, noble metals can be anchored as isolated atoms, either residing on the surface or embedded within the LDH laminates. In 2008, Yan *et al.* utilized DFT technology to explore the feasibility of incorporating various metal cations into LDH laminates[38]. They found that the distortion angle (θ) of octahedral coordination hexahydrate cations $\{[M(H_2O)_6]^{n+}\}$ related to the preferential coordination environment of metal ions significantly influenced the formation of LDH laminates. With an increasing distortion angle, the challenge of incorporating metal cations into LDHs also

escalated. Consequently, only a portion of noble-metal ions, such as Ru, Rh, Ir, and Os (Type I, $\theta < 10°$), could enter the LDH laminates and form well-organized LDHs [Figure 2][36,38]. Conversely, other noble-metal ions, including Ag, Au, Pd, and Pt (Type II, $\theta > 10°$), encounter hindrances in engaging with the formation of LDH laminates due to their enlarged ion radii or the distribution of electron clouds in space unless special synthesis strategies are employed. However, the type of noble metal does not limit the anchoring of noble-metal atoms on the surface of LDH laminates. In this section, we offer a comprehensive overview of the commonly reported synthetic methodologies for LDH-supported noble-metal SACs. Furthermore, we delve into the impact of these diverse strategies on the anchoring positions of noble-metal atoms, explore the underlying mechanisms involved, and analyze the relative advantages and disadvantages of each strategy and their scalability in industrial applications.

Co-precipitation strategy

The co-precipitation strategy involves the direct incorporation of noble-metal salts into the raw materials of LDH during synthesis, enabling the simultaneous formation of LDHs and anchoring of noble-metal atoms within their structure. For Type I noble-metal atoms, namely Ru, Rh, Ir, and Os, which are easy to enter the LDH laminates, there are two possible anchoring positions: (1) within the LDH laminates; (2) on the surface of LDH laminates. For example, Liu *et al.*[39] employed a co-precipitation method to synthesize NiFe-LDH-supported Rh SACs (Rh/NiFe-x) by introducing $RhCl_3·3H_2O$ into the raw materials of NiFe-LDH [Figure 3A and B]. The K-edge X-ray absorption near-edge structure (XANES) simulation, extended X-ray absorption fine structure (EXAFS) spectra fitting and DFT calculations revealed that Rh species were atomically dispersed within NiFe-LDH laminates and coordinated with 5.91 oxygen atoms. However, in another case, Sun *et al.* introduced $RuCl_3·xH_2O$ into the raw materials of Ni_3V-LDH and obtained Ni_3V-LDH-supported Ru SACs (Ru/Ni_3V-LDH) through the hydrothermal method [Figure 3C and D][40]. They indicated that Ru single-atom sites (RuO_4) were anchored on the surface of Ni_3V-LDH laminates by DFT calculation. Compared to doping in Ni_3V-LDH laminates, the formation energy of Ru single-atom sites anchored on the surface of Ni_3V-LDH laminates was much lower. However, the current approach for determining the anchoring positions of noble-metal single atoms starts with XAS coordination data, which can correspond to multiple models. DFT calculations are subsequently applied to pinpoint the most likely models. Since XAS is a bulk-averaging technique, the data may reflect an average of different single-atom sites and involve some fitting errors, contributing to uncertainty in the conclusion of the anchoring positions of noble-metal single atoms.

Type II noble-metal atoms, including Pd, Ag, Pt, and Au, with larger ion sizes, tend to anchor on the surface of LDH laminates by the co-precipitation strategy. A notable example can also be found in the research conducted by Shen *et al.*[41]. They successfully synthesized MgAl-LDH-supported Au SACs (Au_1-MgAl-LDH) utilizing co-precipitation techniques, wherein $HAuCl_4·3H_2O$ was introduced into the raw material of MgAl-LDH [Figure 3E and F]. The Au (> +3) single-atom sites were anchored on the top of Al sites on the surface of MgAl-LDH with the AuO_4 configuration. In addition, Yu *et al.*[42] deposited Pt_{SA}-NiCo-LDH on the surface of nickel foam by co-electrodeposition at a constant potential, wherein K_2PtCl_4 and the raw material of NiCo-LDH were added together in the electrolyte [Figure 3G and H]. The Pt single-atom sites (Pt-O_5) with a valence of approximately +4 were anchored on the surface of NiCo-LDH.

Compared to other synthesis strategies, the co-precipitation strategy has unique advantages in its simple synthesis process. The co-precipitation strategy is straightforward and scalable, making it suitable for large-scale industrial applications. However, due to the strict requirements for reaction conditions such as pH, temperature, potential, and precipitation rate, scaling up may require more advanced control systems to maintain product uniformity and quality consistency.

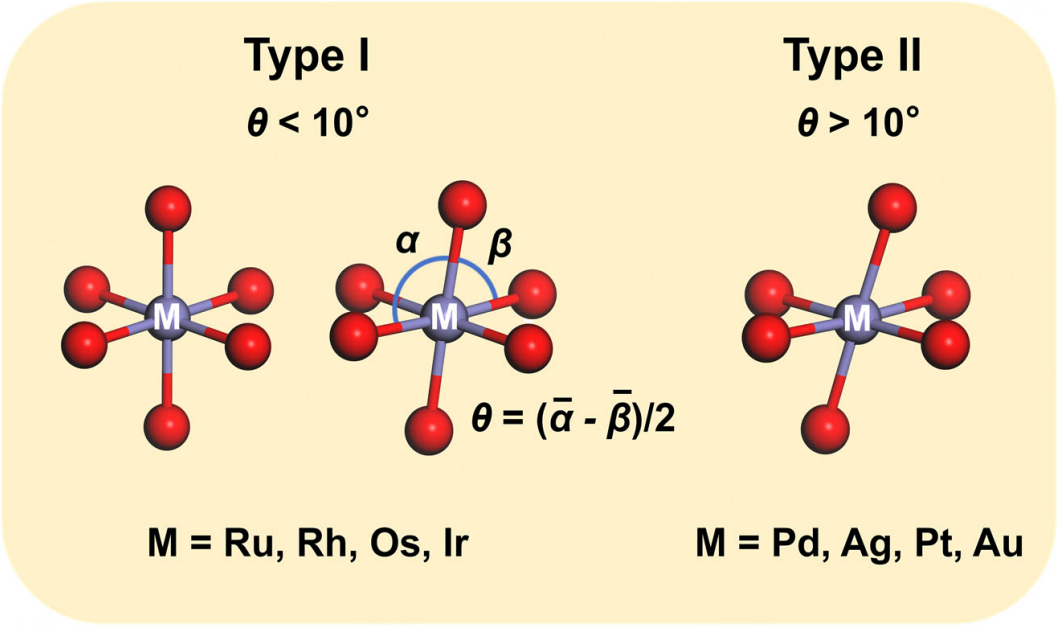

Figure 2. The distortion angle (θ) of the $[M(H_2O)_6]^{n+}$.

Impregnation strategy

Impregnation strategy refers to immersing the pre-synthesized LDHs in a solution containing noble-metal salts so that noble-metal atoms gradually anchor to the surface of LDH laminates. A reduction process is usually required to enhance the anchoring strength of noble-metal single-atom sites. Given that the surface of LDH laminates is enriched with hydroxyl groups, noble-metal atoms could be anchored on the surface as single atoms by these surface hydroxyl groups easily by this strategy. This method serves as a versatile synthetic strategy that can be applied to both type I and type II noble metals. By this impregnation strategy, our group successfully anchored several noble-metal atoms, involving Ru and Pt single-atom sites, onto the surface of LDH laminates[43-46].

For instance, Ru_1/LDH was synthesized by immersing MgAl-LDH in $RuCl_3$ aqueous solution to anchor Ru single atoms and subsequent reduction by H_2/Ar at 100 °C [Figure 4A and B]. The fitting results of EXAFS spectra indicated that the Ru single-atom sites were anchored on the surface of MgAl-LDH in the form of RuO_3. Adding alkali in the impregnation solution can also effectively promote the anchor of noble-metal atoms on the surface of LDH laminates. For example, CoFe-LDH-supported Ru SACs were synthesized by Li *et al.* using this strategy [Figure 4C and D], revealing a valence state between 0 and +3, and a specific coordination environment of RuO_4 for Ru species on the surface of LDH laminates[47]. Hu *et al.*[48] utilized this strategy to anchor Ir single-atom sites on the surface of NiFe-LDH laminates at 80 °C using H_2IrCl_6 as a noble-metal source [Figure 4E and F]. XNANES and EXAFS spectra showed the oxidation state (> +3) and specific configurations of the Ir as IrO_6, while the DFT calculation results indicated that the Ir atoms were placed at the top of the Fe sites. In addition, Chen *et al.*[49] introduced $PtCl_6^{2-}$ in the interlayer of Ni_3Fe-LDH via the impregnation strategy and anchored Pt single-atom sites on the Ni_3Fe-LDH laminates (Ni_3Fe-CO_3^{2-} LDH-Pt SA) via subsequent electrochemical reduction in alkali solution [Figure 4G and H].

The impregnation method offers several advantages in material preparation, such as simplicity, broad applicability, and strong controllability. By adjusting solution concentration and impregnation time, the loading of active components can be precisely controlled. However, this method also has drawbacks,

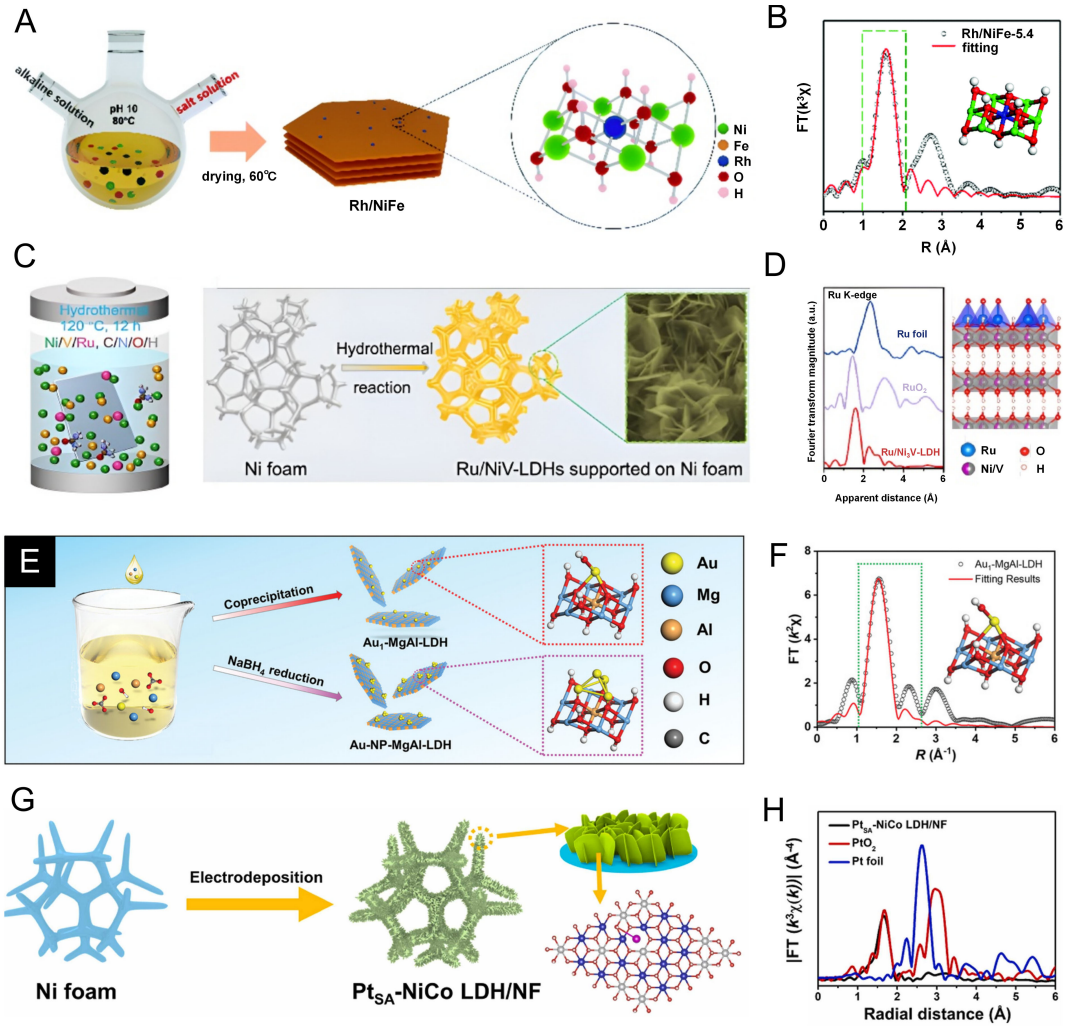

Figure 3. (A, B) Synthesis process (A) and Rh K-edge EXAFS fitting result (B) of Rh/NiFe-x[39]. Copyright 2021, Royal Society of Chemistry; (C, D) Synthesis process (C) and Ru K-edge EXAFS spectra of Ru/Ni_3V-LDH with proposed model (D)[40]. Copyright 2022, American Chemical Society; (E, F) Synthesis process (E) and Au L_3-edge EXAFS fitting results (F) of Au_1-MgAl-LDH[41]. Copyright 2023, Wiley-VCH; (G, H) The synthesis process (G) and Pt L_3-edge EXAFS spectra (H) of Pt_{SA}-NiCo-LDH/NF[42]. Copyright 2023, Elsevier. LDHs: Layered double hydroxides; EXAFS: Extended X-ray absorption fine structure; Pt_{SA}-NiCo-LDH/NF: Pt single-atom sites (PtO_5) anchored NiCo-LDH supported by nickel foam.

including the potential uneven distribution of active components, the need for strict control of solvent selection, and the complexity and time costs associated with multiple steps. Therefore, achieving consistency and reproducibility in large-scale production can be challenging.

Ion exchange strategy

The ion exchange strategy involves the substitution of metal cations in the LDH laminates with noble-metal cations by post-synthesis strategies, which anchor noble-metal atoms within the LDH laminates. During a cation exchange reaction, the exchanged cations undergo migration from the host lattice and subsequent dissolution in the solvent, whereas the substituted cations migrate into the host lattice[50]. The cation exchange reaction possesses two main driving forces: (1) mass-driven law caused by the concentration of highly substituted cations (Le Chatelier's principle); (2) the difference in solubility between the reactant and product[51]. For instance, Mu *et al.*[52] harnessed the Ru to replace a portion of transition-metal atoms within

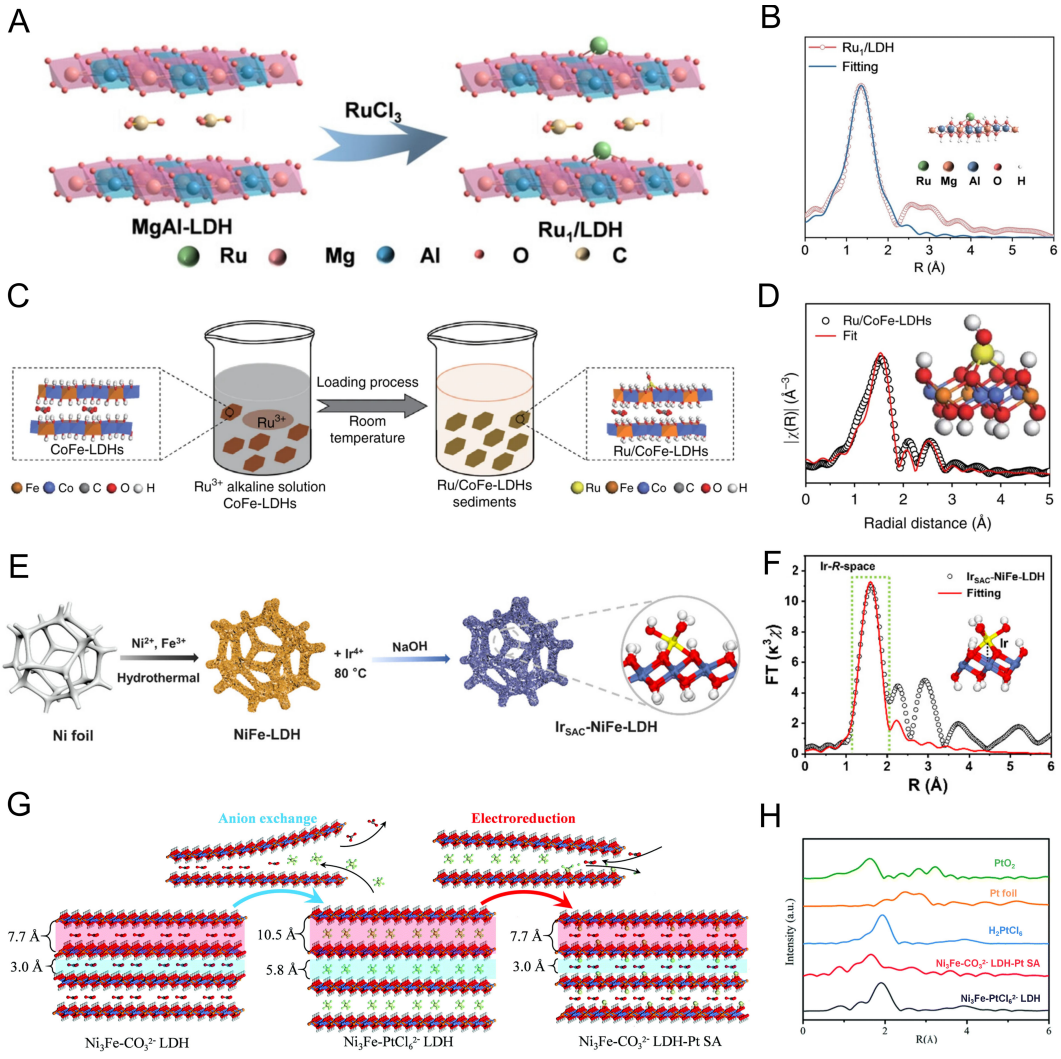

Figure 4. (A, B) Synthesis progress (A) and Ru K-edge EXAFS fitting curve (B) of Ru_1/LDH[43]. Copyright 2023, Wiley-VCH; (C, D) Synthesis progress (C) and Ru K-edge EXAFS fitting curve (D) of Ru/CoFe-LDH[47]. Copyright 2019, Springer Nature; (E, F) Synthesis progress (E) and Ir L_3-edge EXAFS fitting curve (F) of Ir_{SAC}-NiFe-LDH[48]. Copyright 2023, American Chemical Society; (G, H) Synthesis progress (G) and Pt L_3-edge EXAFS spectra (H) of Ni_3Fe-CO_3^{2-} LDH-SA[49]. Copyright 2021, Royal Society of Chemistry. LDHs: Layered double hydroxides; EXAFS: Extended X-ray absorption fine structure.

FeCo-LDH laminates (Ru_1SACs@FeCo-LDH) by soaking the FeCo-LDH in ethanol solution with a high concentration of $RuCl_3$ [Figure 5A and B]. Ru_1SACs@FeCo-LDH not only retained the porous structure of FeCo-LDH but also exhibited a distinctive symmetry-breaking structure formed by the asymmetric coordination of Fe/Co atoms around Ru atoms. The ion exchange strategy diverges from the impregnation strategy mentioned earlier in its demand for a notably elevated concentration of noble-metal salts to facilitate the cation exchange reaction.

In addition, transition-metal atoms within LDH laminates have been found to detach into the solution during the electrochemical process in prior studies[53,54]. Although this phenomenon results in the loss of active sites[55], it also presents an opportunity for the incorporation of noble-metal atoms into LDH laminates. Interestingly, this strategy can achieve ion exchange between type II noble-metal ions and transition metal ions within the LDH laminates. For instance, He *et al.*[56] achieved ion exchange of Ni and

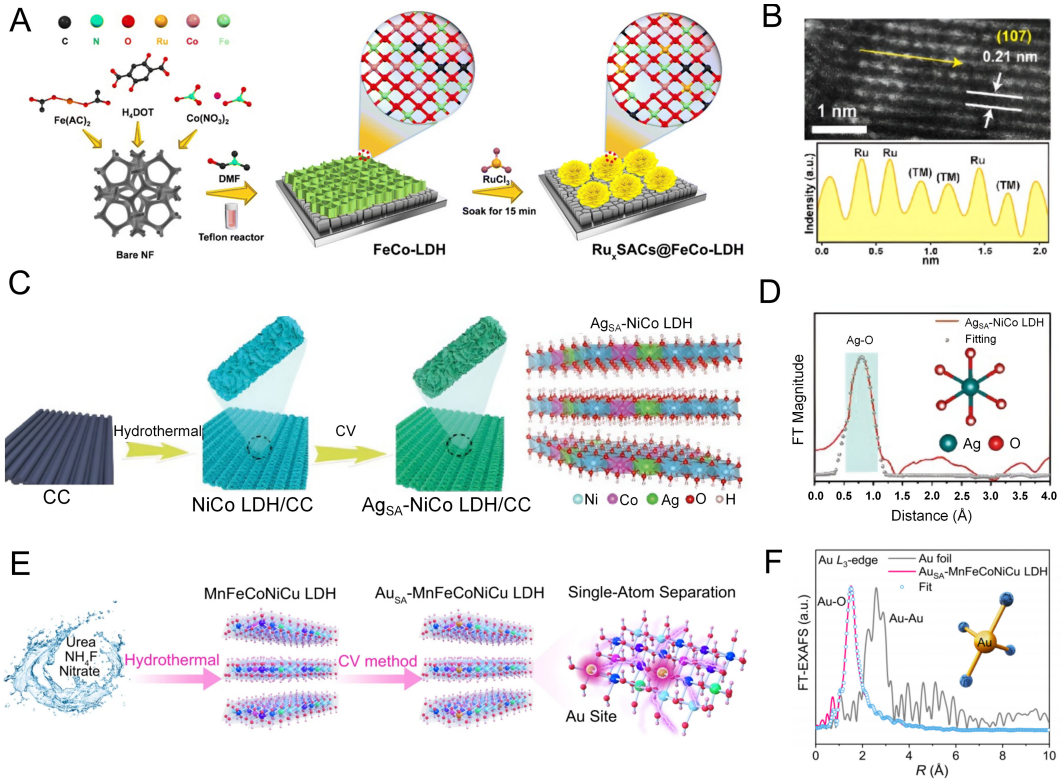

Figure 5. (A, B) Synthesis progress (A) and AC HAADF-STEM image with linear scanning analysis (B) of Ru_1SACs@FeCo-LDH[52]. Copyright 2022, Royal Society of Chemistry; (C, D) Synthesis progress (C) and Ag K-edge EXAFS fitting curve (D) of Ag_{SA}-NiCo-LDH/CC[56]. Copyright 2023, Wiley-VCH; (E, F) Synthesis progress (E) and Au L_3-edge EXAFS spectra fitting curve (F) of Au_{SA}-MnFeCoNiCu-LDH[57]. Copyright 2023, Springer Nature. SACs: Single-atom catalysts; LDHs: Layered double hydroxides; AC HAADF-STEM: Aberration-corrected high-angle annular dark-field scanning transmission electron microscopy; EXAFS: Extended X-ray absorption fine structure.

Ag in NiCo-LDH (Ag_{SA}-NiCo-LDH/CC) via the cyclic voltammetry (CV) method [Figure 5C and D]. The Ag single-atom sites were dispersed in the NiCo-LDH laminates in the valence state between 0 and 1 and the coordination form of AgO_6. Wang *et al.*[57] also anchored Au single-atom sites onto Fe vacancies in MnFeCoNiCu-LDH using the electrochemical CV method [Figure 5E and F]. They confirmed the atomic dispersion and coordination environment (AuO_4) of Au species via the inductively coupled plasma-optical emission spectroscopy (ICP-OES), AC HAADF-STEM, EXAFS, and DFT techniques. We speculate that the main reason for Au and Ag entering LDH laminates is due to the surface defects and strain in the LDH laminates caused by the separation of transition metal cations during the electrochemical CV process. The surface defects and strain are considered to be ideal high-energy sites for cation exchange reactions[58]. The ion exchange strategy offers significant advantages, such as high selectivity, allowing for the precise anchor of noble-metal atoms within LDH laminates, thereby achieving uniform distribution of noble-metal single-atom sites. This strategy typically operates under mild conditions, making it relatively simple and easy to control. However, in LDH laminates, certain metal ions are highly stable and difficult to exchange, which may limit the diversity of anchoring positions for noble-metal single-atom sites, hinder activity regulation, and pose challenges for industrial-scale production.

THE MICROENVIRONMENT REGULATION STRATEGIES OF LDH-SUPPORTED NOBLE-METAL SACS

The microenvironment of SACs refers to the localized, specific, and isolated chemical environment surrounding the central metal atoms. This includes factors such as coordination environments and electronic configuration[59-63]. Precisely regulating these microenvironments is of utmost importance, as it holds the key to unlocking unprecedented catalytic efficiency and selectivity, thereby paving the way for sustainable and environmentally friendly chemical processes[64-67]. The regulation of microenvironments is pivotal in deciding the catalytic performance of SACs by influencing the electronic state of the active metal, thus impacting the overall catalytic activity. Inheriting the highly tunable structure of LDHs, LDHs are not only excellent supports for SACs but also are beneficial for precise regulation of the microenvironments of noble-metal single-atom sites. In this section, we have summarized the reported microenvironment regulation strategies of LDH-supported noble-metal SACs [Figure 6], including defect engineering strategy and axial coordination engineering strategy.

Defect engineering strategy

In SACs, the pronounced interaction or charge transfer between the metal atoms and the supports, known as the metal-support interaction, is evident[68]. The strong metal-support interaction can capture and stabilize metal atoms, and also provides a new opportunity to regulate the electronic structure and coordination environment of metal atoms, thereby optimizing their catalytic performance[69]. An effective strategy for regulating metal-support interactions is introducing defects into the supports, known as the defect engineering strategy. Defects are widely present in nanomaterials, serving as effective anchoring sites for metal atoms and an important component of the microenvironment of central metal atoms[61,70]. Pre-constructing defect sites on the supports to construct single-atom sites with defined microenvironments is one of the most popular synthesis routes for SACs[71]. Recently, targeted defect engineering in LDHs has achieved extensive development[72,73], which endows the possibility to attain precise directional anchoring of noble-metal single-atom sites on the LDH laminates, thereby achieving directional control of the single-atom microenvironment.

Recently, our group has developed a defect engineering strategy to construct noble-metal single-atom sites with a specific microenvironment directionally. Specifically, divalent/trivalent cation vacancies on NiFe-LDH were prepared by doping alkali-soluble Zn/Al in the LDH laminates[44]. Subsequently, Ru single atoms were accurately deposited in these cation vacancies by an impregnation-reduction process, labeled as Ru_1/LDH-V_{II} and Ru_1/LDH-V_{III} [Figure 7A and B]. The coordination environments of the Ru single-atom sites differ between Ru_1/LDH-V_{III} and Ru_1/LDH-V_{II}, specifically in their second coordination shell. In Ru_1/LDH-V_{III}, only Ru-O-Ni bonds were present, whereas in Ru_1/LDH-V_{II}, both Ru-O-Ni and Ru-O-Fe bonds coexisted. DFT calculations indicated that Ru atoms positioned atop Fe sites exhibited greater stability compared to those on Ni or O sites of the NiFe-LDH. Notably, the Ru single-atom sites incorporated into the LDH laminates coordinated with six oxygen atoms, a coordination geometry consistent with that of the transition metals within the LDH laminates.

The noble metals that pose challenges in entering the LDH laminates can also be precisely anchored on the surface of LDH laminates using this defect engineering strategy. For instance, Pt single-atom sites were precisely anchored onto the top of the divalent cation vacancies of CoFe-LDH with divalent cation vacancies (Pt_1/LDH_v) [Figure 7C and D] by a similar process[45]. The Pt atoms in the Pt_1/LDH_v were coordinated with three oxygen atoms, while Pt_1/LDH prepared by impregnation method on CoFe-LDH without vacancies only coordinated with one oxygen atom. These structural differences resulted in significant differences in their intrinsic properties. The defect engineering strategy can achieve targeted

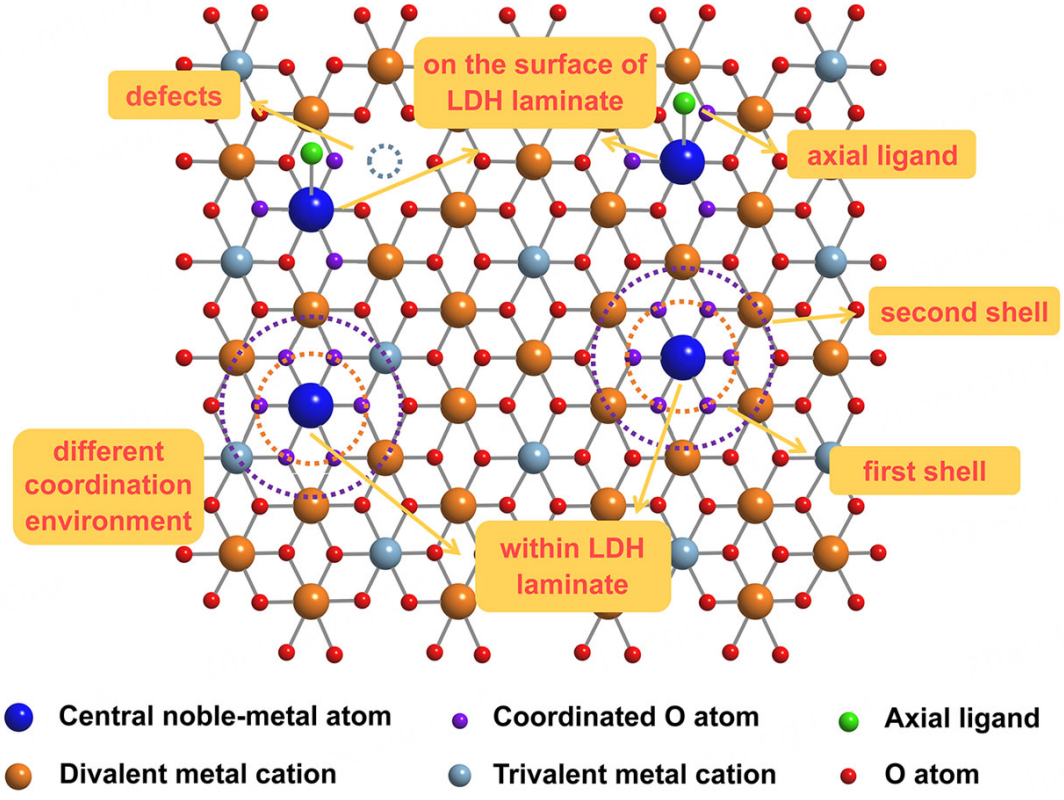

Figure 6. The microenvironment of noble-metal single-atom sites. LDHs: Layered double hydroxides.

anchoring of noble-metal atoms with a specific microenvironment, providing a novel route for the precise synthesis of SACs with bright development prospects. Besides the targeted anchoring of noble-metal atoms, defect engineering strategies can serve as a post-treatment approach to regulate the interaction between noble-metal atoms and LDH laminates. For example, Zhai *et al.*[74] employed an alkaline etching method to remove Al from NiFeAl-LDH anchored with Ru single-atom sites [Figure 7E and F], yielding a defective (D-) NiFe-LDH anchored with RuO_4 sites (Ru_1/D-NiFe-LDH). Experimental results demonstrated that the introduction of metal defects significantly enhanced the interaction between Ru atoms and LDH laminates.

Axial coordination engineering strategy

The coordination structure and geometric configuration of SACs are pivotal factors influencing the catalytic activity of central metal atoms[75]. Axial coordination engineering is a novel approach for adjusting the local microenvironment of central metal atoms in SACs[76]. By incorporating one or more ligands at the axial positions of the central metal atoms, the planar symmetry of SACs is intentionally broken, achieving changes and adjustments in the electron distribution of central metal atoms[77]. Recently, axial coordination engineering has also been applied in LDH-supported noble-metal SACs.

We have developed a simple irradiation impregnation method to directionally manipulate the axial ligands on the Pt single-atom sites (labeled as X-Pt/LDH, X = F, Cl, Br, I, and OH) supported on the surface of NiFe-LDH [Figure 8A and B][46]. Specifically, by immersing the synthesized Cl-Pt/LDH in KOH aqueous solution with white light irradiation, HO-Pt/LDH was obtained. When immersing the obtained OH-Pt/LDH in 2 M NaX solution, its OH axial ligand underwent an exchange with X. This allowed us to achieve diverse axial ligand coordination for the Pt single-atom sites, where each Pt atom was coordinated

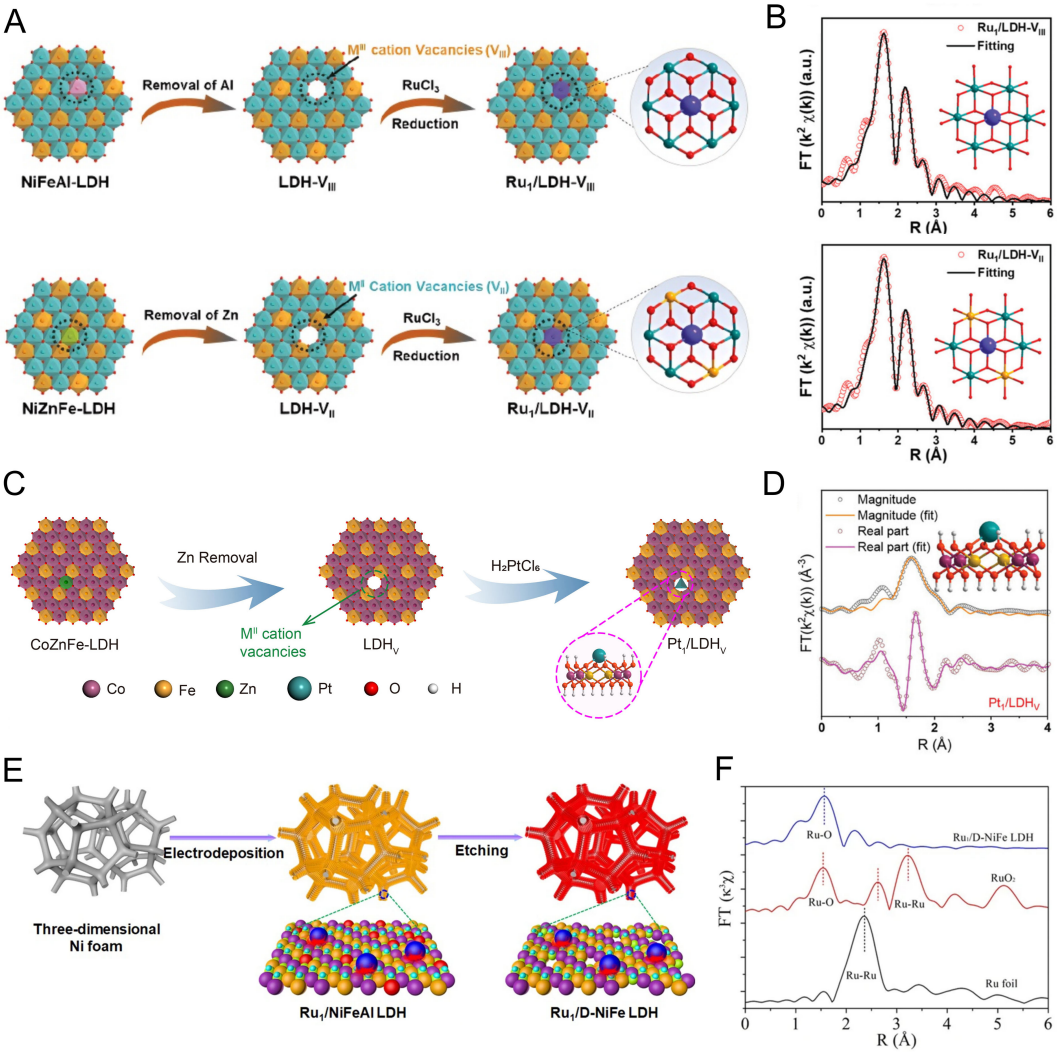

Figure 7. (A, B) Synthesis progress (A) and Ru K-edge EXAFS fitting curves (B) of Ru_1/LDH-V_{III} and Ru_1/LDH-V_{II} [44]. Copyright 2022, Wiley-VCH; (C, D) Synthesis progress (C) and Pt L_3-edge EXAFS fitting curve (D) of Pt_1/LDH_V [45]. Copyright 2024, Wiley-VCH; (E, F) Synthesis progress (E) and Ru K-edge EXAFS fitting curves (F) of Ru_1/D-NiFe-LDH [74]. Copyright 2021, Springer Nature. LDHs: Layered double hydroxides.

with three O atoms and one X atom. The above analysis results were proved by AC HAADF-STEM, XAS, far-infrared spectra, ultraviolet-visible diffuse reflectance spectroscopy (UV-vis DRS) spectra, electron paramagnetic resonance (EPR) spectra, and X-ray photoelectron spectra (XPS). Duan *et al.*[78] introduced a mixture of dilute solutions of NaOH and $IrCl_3$ to CoFe-LDH dispersion liquid to anchor Ir single-atom sites on the surface of CoFe-LDH (Ir/CoFe-LDH) and facilitated the adjustment of Cl ligands at Ir single-atom sites [Figure 8C and D]. The valence state of Ir single-atom sites was higher than +4, and their coordination numbers with O and Cl were 3.1 and 2.5, respectively.

Besides these two widely studied strategies, the microenvironment of LDH-supported noble-metal SACs can be regulated by substituting the metal in LDH laminates. For example, Duan *et al.*[79] substituted Ni^{2+} in NiFe-LDH with Fe^{2+} ($NiFe^{2+}$Fe-LDH) to modulate the interaction between Ru atoms and the LDH laminates. For comparison, they anchored Ru single-atom sites on $NiFe^{2+}$Fe-LDH (Ru/$NiFe^{2+}$Fe-LDH) and NiFe-LDH (Ru/NiFe-LDH) under the same conditions. Experimental results demonstrated that the

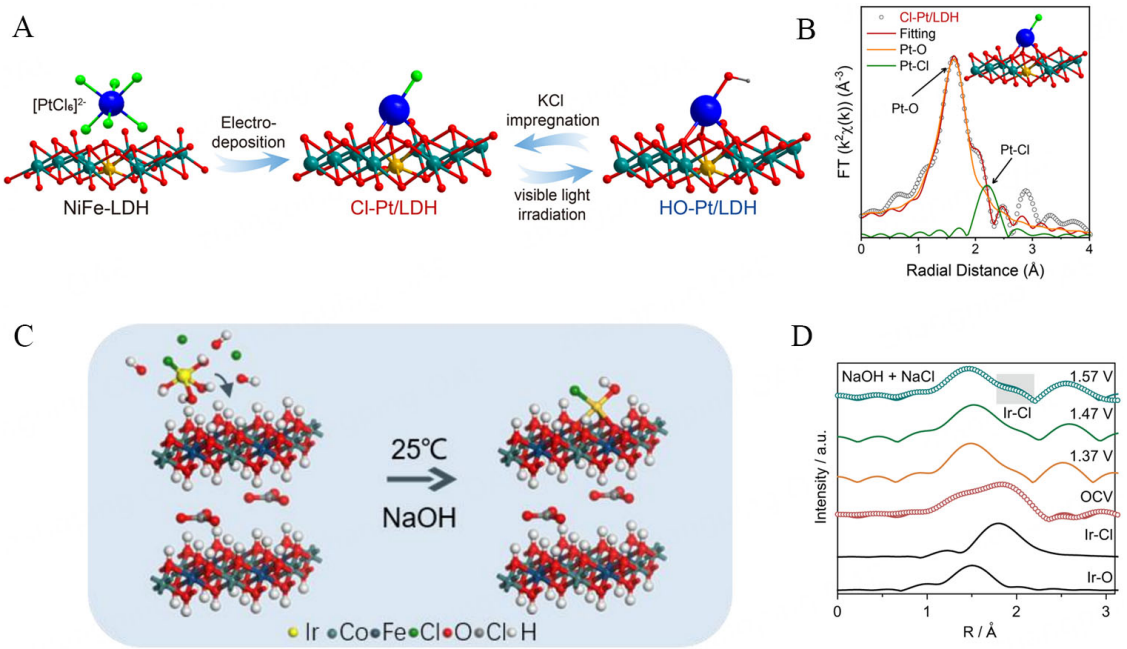

Figure 8. (A, B) Synthesis progress (A) and Pt L_3-edge EXAFS fitting curves (B) of Cl-Pt-LDH[46]. Copyright 2022, Springer Nature; (C, D) Synthesis progress (C) and in situ EXAFS spectra (D) of Ir/CoFe-LDH[78]. Copyright 2024, Springer Nature. LDHs: Layered double hydroxides; EXAFS: Extended X-ray absorption fine structure.

reducibility of Fe^{2+} enhanced the anchoring ability of the LDH supports to Ru atoms, resulting in Ru loading on Ru/NiFe^{2+}Fe LDH being three times higher than that on Ru/NiFe LDH. Moreover, the reducibility of Fe^{2+} decreased the oxidation state of Ru (from 2.58 to 2.37) and kept it at a lower level throughout the entire working process. Despite recent attention from researchers on microenvironment regulation in LDH-supported noble-metal SACs, reports on this topic remain scarce, highlighting the need for further exploration. Following our overview of microenvironment regulation strategies of LDH-supported noble-metal SACs, we also provide an introduction to their characterization techniques.

THE CHARACTERIZATION TECHNIQUES OF LDH-SUPPORTED NOBLE-METAL SACS

The significant advancements in characterization techniques have been crucial in driving the success of SACs in the field of catalysis. Confirming the existence of noble-metal single-atom sites and acquiring detailed information about their microenvironment are essential for unveiling the structure-performance relationship in LDH-supported noble-metal SACs and for the subsequent development of high-performance LDH-supported noble-metal SACs. However, this process is undoubtedly challenging. At present, researchers predominantly employ a combination of AC HAADF-STEM, XAS, and DFT calculations to carry out in-depth investigations of LDH-supported noble-metal SACs. In this section, we have summarized the advantages and limitations of the aforementioned characterization techniques.

AC HAADF-STEM technique

Since the 1990s, advancements in electron microscopy have led to significant improvements in aberration-corrected scanning transmission electron microscopy (AC-STEM) technology with sub-angstrom resolution[34]. Particularly, the application of high-angle annular dark-field (HAADF) imaging mode has enabled the precise visualization of individual metal atoms, which has greatly advanced research and applications in the field of nanomaterials. In HAADF images, the brightness of spots corresponding to metal atoms is typically proportional to their atomic number, which allows for the effective differentiation

between LDH supports and noble-metal atoms. However, it is important to recognize that AC HAADF-STEM technology has certain limitations. AC HAADF-STEM has difficulty distinguishing between metal atoms with similar atomic masses[80], such as Ni and Fe, which are commonly found in LDH laminates, as well as noble metals such as Pt and Au. Moreover, AC HAADF-STEM is limited in its ability to conclusively verify the absolute uniformity of single-atom sites on the support, as AC HAADF-STEM images reflect only a fraction of the sample. Therefore, AC HAADF-STEM is often combined with XAS, a bulk-averaging technique, to assess the absolute uniformity of single-atom sites on the support across the entire sample.

XAS technique

Beside visualizing individual metal atoms, understanding how their local microenvironment, including coordination and support interactions, is also crucial to SACs, as it impacts their activity and stability. XAS is widely utilized due to its element-specific nature and ability to investigate the electronic and atomic structure of examined atoms[81]. It can be divided into XANES and EXAFS regions. Details about the oxidation state, electronic properties, and bonding geometry of absorbing atoms are generally derived from analyzing the XANES region. Concurrently, analysis of the EXAFS region provides in-depth information on the microenvironment of single-atom sites, including the types, numbers, and bond lengths of neighboring atoms, typically within a range of ~ 5Å. However, XAS technology also has its limitations. The limitations of EXAFS fitting primarily stem from its indirect nature and inherent subjectivity. Structural information is inferred by fitting with a hypothesized model rather than being directly obtained. The choice of the structural model and the fitting process may involve subjective judgments, which can undermine the reliability of the results. Furthermore, coordination number errors in the fitting process can reach up to 10%, further reducing the accuracy of the structural interpretation[82]. Identifying specific coordination elements in unknown samples, especially when peaks with similar bond lengths are present in the R space, can be particularly difficult[19]. And the reliability of fitting results can be compromised by the low quality of EXAFS in many XAS datasets. Furthermore, as a bulk-averaging technique, XAS provides information that represents an average value[83]. However, this value is often assumed to reflect the unique configuration of single-atom sites within the sample, though it may be an average of different configurations of single-atom sites. XAS technology is frequently paired with DFT calculations to determine the microenvironmental structure of single-atom sites, enhancing the reliability of the results.

DFT calculations

Compared to AC HAADF-STEM and XAS techniques, DFT calculations offer the advantage of investigating catalysts at a more microscopic scale. Typically, DFT is employed to predict the possible adsorption sites of metal atoms, which are generally the local coordination structures with the lowest formation energy and highest stability[84]. By integrating these predictions with the coordination information obtained from XAS, the most likely configurations of single-atom sites can be inferred. Additionally, DFT calculations can simulate the adsorption of reaction intermediates and the energy barriers of different reaction pathways to analyze reaction mechanisms and assess charge transfer during catalytic processes. Combining DFT calculations with experimental characterization enhances the accuracy and reliability of research conclusions. However, DFT simulations rely on idealized models that do not fully capture the complexities of real-world conditions. As a result, current findings in SAC research retain a degree of uncertainty, primarily due to the limitations of existing technologies. Nevertheless, it is anticipated that as characterization techniques continue to advance, SAC research will experience significant breakthroughs. Following our overview of the characterization techniques of LDH-supported noble-metal SACs, we also provide a review of the applications of LDH-supported noble-metal SACs.

THE APPLICATIONS OF LDH-SUPPORTED NOBLE-METAL SACS

LDH-supported noble-metal SACs embody the combined strengths of LDHs and noble metals, showing excellent performance in electrocatalysis, thermal catalysis, photocatalysis, *etc.*[85,86]. This section discusses the LDH-supported noble-metal SACs used in electrocatalytic water splitting, hybrid water electrolysis, hydrogenation, selective oxidation, hydrosilylation, photocatalytic benzene oxidation, and enzyme-like applications.

Electrocatalysis

Excessive reliance on fossil fuels has brought increasingly severe energy crises and environmental issues for humanity[87]. Hence, the exploration and development of renewable energy conversion devices have emerged as a research hotspot to address these challenges. Electrocatalysis is extensively used in producing clean fuels, green chemical synthesis, and reducing carbon emissions[88,89]. Currently, LDH-supported noble-metal SACs have been widely explored and applied in electrocatalytic water splitting and hybrid water electrolysis.

Electrocatalytic water splitting to produce green hydrogen stands out as one of the most promising approaches for efficiently utilizing intermittent renewable energy and achieving decarbonization in the future[90,91]. The water splitting involves two crucial half-reactions: the oxygen evolution reaction (OER) and the hydrogen evolution reaction (HER)[92]. Noble-metal-based catalysts involving Pt, Ru, and Ir are commercial electrocatalysts for water splitting[85,93]. However, their heavy expense and limited availability hamper the prevalent commercial deployment of such technologies. Decreasing the size of noble-metal catalysts from particles to individual atoms can effectively boost the utilization of noble metals to offset their high prices. Therefore, LDH-supported noble-metal SACs have attracted great attention[94]. Up to now, LDH-supported noble-metal SACs have achieved rapid development in electrocatalytic water splitting.

As the anode reaction, the OER is vital in the water splitting. Zhang *et al.*[95] synthesized NiFe-LDH with surface-anchored Au single-atom sites (AuO), named ^{s}Au/NiFe-LDH, which exhibited a 6-fold OER activity improvement (an overpotential of 198 mV at 129.8 mA cm^{-2}) by 0.4 wt% Au loading [Figure 9A-E]. In-situ Raman characterizations revealed that the active sites were attributed to Ni rather than Au as only the Ni sites underwent electrochemical reconstruction during the CV cycle. The introduction of Au led to the redistribution of charges between Au and LDH with a net charge difference of 0.32e, which was subsequently transferred to neighboring O, Ni, and Fe atoms. This facilitated the adsorption of OH^- ions and modified the adsorption strength of O* and OOH* intermediates, leading to decreased energy barriers during the rate-limiting step from O* to OOH*.

Besides the role in regulating the active sites of OER, noble-metal atoms are widely recognized as the main catalytic active sites. Li *et al.* anchored Ru single-atom sites (RuO_4) on the surface of CoFe-LDH (Ru/CoFe-LDH) to achieve a catalyst with high activity and stability in OER [Figure 9F-I][47]. This Ru/CoFe-LDH displayed a lower overpotential of 198 mV at 10 mA cm^{-2} (η_{10}) and superior stability (99% origin current density after 24 h) compared with CoFe-LDH and RuO_2. In-situ XAS demonstrated that the electronic interaction between Ru and LDHs maintained the oxidation state of Ru below 4+ throughout the entire electrochemical process, a critical factor contributing to its exceptional activity and stability. DFT + U calculations also demonstrated the significant electron coupling synergy between Ru atoms and LDHs material enhanced the activity and stability of OER by achieving optimal adsorption-free energy for *OOH species while preventing the formation of highly oxidized Ru states. Very recently, the same group developed an Ir SACs (RuO_3Cl_2) on CoFe-LDH (Ir/CoFe-LDH) that possessed excellent performance in alkaline seawater electrolysis by controlling the chloride adsorption and fine-tuning the electron distribution of the Ir atoms[78]. Remarkably, the Ir/CoFe-LDH demonstrates exceptional OER activity in a

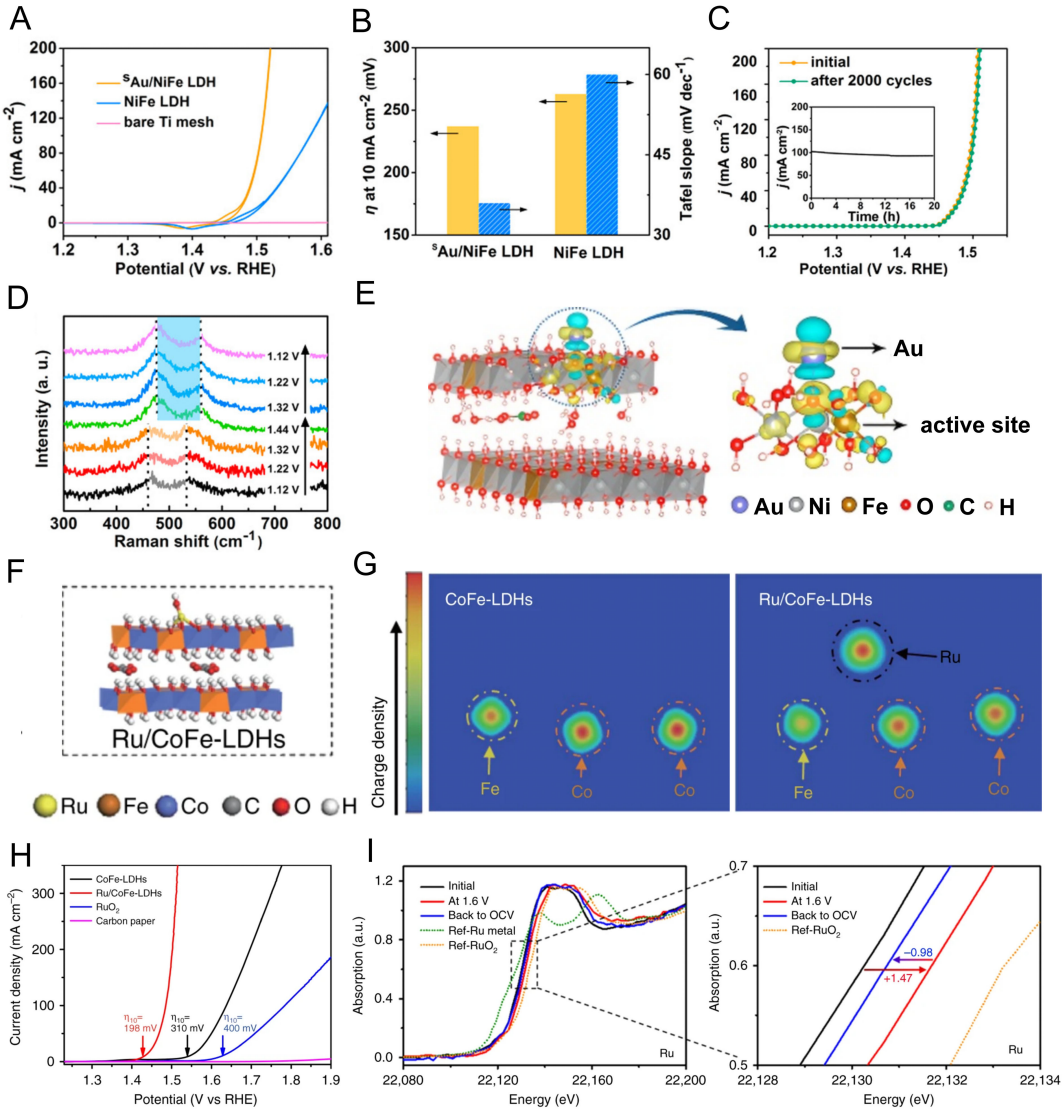

Figure 9. (A) CV curves of different catalysts; (B) Overpotential and Tafel slope of different catalysts; (C) LSV curves of ^{S}Au/NiFe-LDH before and after 2000 cycles and the time-dependent current density; (D) Raman spectra of ^{S}Au/NiFe-LDH at various potentials; (E) Differential charge densities of NiFe-LDH with/without Au atom[95]. Copyright 2018, American Chemical Society; (F) The model of Ru/CoFe-LDH; (G) Differential charge density of elements in CoFe-LDH and Ru/CoFe-LDH; (H) The OER curves of different catalysts; (I) In-situ XANES of Ru/CoFe-LDH[47]. Copyright 2019, Springer Nature. LDHs: Layered double hydroxides; CV: cyclic voltammetry; RHE: reversible hydrogen electrode; LSV: linear scan voltammetry.

6 M NaOH + 2.8 M NaCl electrolyte, achieving a 202 mV overpotential. Furthermore, it maintains 100% selectivity and remarkable stability at high current densities (400-800 mA cm^{-2}) over 1,000 h. Experimental characterization and DFT calculations demonstrated that the dynamic adjustment of OH and Cl coordination on Ir in Ir/CoFe LDH during operation significantly enhanced the adsorption of *OOH intermediates, thereby lowering the energy barrier for *OOH formation.

Furthermore, precise manipulation of the axial ligands in noble-metal SACs offers a powerful means to fine-tune their catalytic activity. By carefully adjusting the coordination microenvironment, our group significantly enhanced the performance of HER electrocatalysts of Pt single atoms (PtO_3X) anchored on NiFe-LDH nanoarrays [Figure 10A-F][46]. We implemented Pt single-atom sites with diverse axial ligands

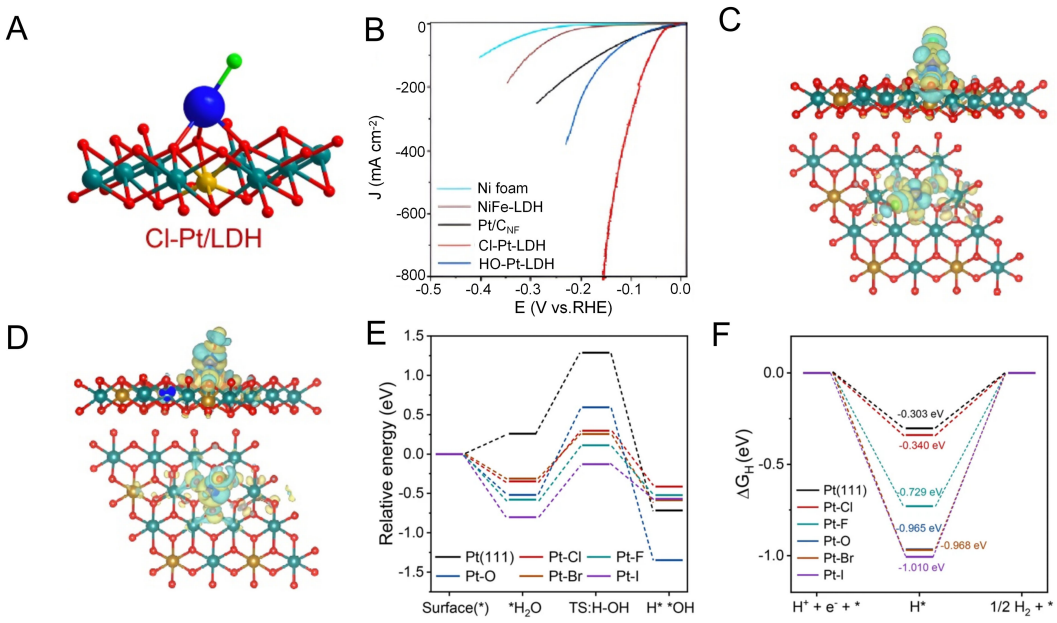

Figure 10. (A) The model of Cl-Pt/LDH; (B) HER curves of different catalysts; Computational models and localized electric field distributions of (C) Cl-Pt-LDH and (D) HO-Pt-LDH; (E) Energy barriers for water dissociation and (F) adsorption-free energies of H* on different catalysts[46]. Copyright 2022, Springer Nature; LDHs: Layered double hydroxides; HER: hydrogen evolution reaction; RHE: reversible hydrogen electrode.

such as F, Cl, Br, I, and OH on NiFe-LDH nanoarrays by a facile irradiation-impregnation strategy. During electrocatalytic HER, Cl-Pt/LDH demonstrated superior activity, achieving a remarkably low overpotential of just 25.2 mV at 10 mA cm^{-2}, overbeating Pt SACs with other axial ligands. DFT calculations revealed that alterations in the axial ligands surrounding Pt atoms induced substantial charge redistribution, impacting the adsorption strength of Pt atoms on alkaline HER intermediates like water adsorption, water dissociation, *OH desorption, and the conversion from *H to H_2. Pt with Cl axial ligand exhibited the lowest energy barrier among these processes. The performance of Cl-Pt/LDH was assessed in an alkaline water electrolyze based on membrane electrode assembly (MEA) technology, achieving a remarkable energy efficiency of up to 80%. These findings highlight the potential application of LDH-supported noble-metal SACs for efficient hydrogen production in industrial settings.

Apart from serving as single-functional catalysts for OER or HER, LDH-supported noble-metal SACs also present the potential to catalyze both OER and HER concurrently. It is ascribed to the presence of multiple catalytic centers, including noble metal atoms and non-noble-metal atoms within the LDH laminates. These multiple catalytic sites may possess strong electronic interactions with each other, leading to unique catalytic activity and stability. As an example, Sun *et al.*[40] modified Ru atoms (RuO_4) on the surface of Ni_3V-LDH (Ru/Ni_3V-LDH) and achieved excellent HER and OER catalytic performance by utilizing strong electronic interactions between noble-metal atoms and the supports. Ru was the active site of HER, while Ni was the site of OER. Due to the strong metal-supports interaction between Ru and Ni_3V-LDH supports, the oxidation states of Ru and Ni maintained low fluctuations during HER and OER processes, allowing the catalyst to avoid structural restructuring. To gain a comprehensive understanding of the current research, we have outlined the current application of LDH-supported noble-metal SACs in electrocatalytic water splitting, as listed in Table 1.

Table 1. LDH-supported noble-metal SACs for electrocatalytic water splitting

Noble metal	LDH type	Application	Overpotential (mV)	Stability	Ref.
Pt (0.72 wt%)	NiFe-LDH	HER	η_{10}: 25.2	No evident decay over 100 h test at 500 mA cm^{-2}	[46]
Ru (12.8 wt%)	NiV-LDH	HER	η_{10}: 6	No evident decay after 5,000 CV cycles	[96]
Ru (0.45 wt%)	FeCo-LDH	OER	η_{10}: 198	99% current remained after 24 h test at initial 200 mA cm^{-2}	[47]
Ir (8.47 wt%)	NiFe-LDH	OER	η_{10}: 194	No evident decay over 120 h test at 200 mA cm^{-2}	[48]
Ag (0.50 wt%)	NiCo-LDH	OER	η_{10}: 192	94.7% current remained after 500 h test at initial 100 mA cm^{-2}	[56]
Au (1.10 wt%)	MnFeCoNiCu-LDH	OER	η_{10}: 213	93.6% current remained after 700 h test at initial ~ 100 mA cm^{-2}	[57]
Ru (1.32 wt%)	$NiFe^{2+}$Fe-LDH	OER	η_{10}: 194	Increase of 16mV after 100 h test at 100 mA cm^{-2}	[79]
Au (0.40 wt%)	NiFe-LDH	OER	η_{10}: 237	No evident decay after 2,000 CV cycles	[95]
Ir (1.59 wt%)	NiCr-LDH	OER	η_{10}: 232	No evident decay over 36 h test at 1.48 V (*vs.* RHE)	[97]
Ru (9.45 wt%)	NiV-LDH	HER OER	η_{10}: 21 η_{10}: 225	No evident decay over 240 h test at 10 mA cm^{-2} in the system of overall water splitting	[40]
Pt (9.70 wt%)	NiFe-LDH	HER OER	η_{10}: 45 η_{10}: 218	No evident decay over 12 h for HER	[49]
Ru_2 (1.53 wt%) Ru_1 (0.51 wt%)	FeCo-LDH	HER OER	η_{500}: 84 η_{10}: 194	No evident decay over 1,000 h test at 1 A cm^{-2} in the system of overall water splitting	[52]
Ru (1.20 wt%)	NiFe-LDH	HER OER	η_{10}: 18 η_{10}: 189	No evident decay over 100 h test at initial ~ 100 mA cm^{-2} in the system of overall water splitting	[74]
Ru (5.23 wt%)	CoV-LDH	HER OER	η_{10}: 28 η_{25}: 263	Increase of 12 mV in η_{10} after 2,000 CV cycles in the system of overall water splitting	[98]

η_x: Overpotential required when the current density reaches x mA cm^{-2}; LDHs: layered double hydroxides; SACs: single-atom catalysts; HER: hydrogen evolution reaction; OER: oxygen evolution reaction; CV: cyclic voltammetry; RHE: reversible hydrogen electrode.

In traditional water splitting, the sluggish kinetics of OER and low-added-value products pose challenges in reducing the cost of hydrogen through this process. Consequently, researchers have proposed hybrid water electrolysis systems that substitute OER with other reactions, such as alcohol oxidation, which are thermodynamically and economically more favorable[99]. This approach not only decreases the energy consumption and costs in hydrogen production but also yields high-value added oxidation products[100]. In recent years, this emerging technology has garnered significant attention from researchers and has made rapid progress and breakthroughs. LDH-supported noble-metal SACs have also been documented for their application in hybrid water electrolysis systems.

The oxidation of 5-hydroxymethylfurfural (HMF) holds immense significance as it marks a vital transformation process in converting biomass into valuable chemicals, thereby promoting sustainable production of renewable fuels and materials. Xu *et al.*[101] achieved efficient HMF oxidation (HMFOR) via Ru single-atom sites (RuO_4) anchored on the surface of NiFe-LDH ($Ru_{0.3}$/NiFe) via electrodeposition strategy. Compared with OER [1.13 V *vs.* reversible hydrogen electrode (RHE)], $Ru_{0.3}$/NiFe possessed a lower onset potential at 0.1 mA cm^{-2} (0.91V) in HMFOR with the oxidation product of 2,5-furan dicarboxylic acid (FDCA), at a yield of 98.68%. Moreover, both experiment and DFT results suggested that the incorporation of Ru single-atom sites improved the adsorption energy of HMF, thus enhancing the capacity of FeNiOOH to capture protons and electrons.

Bifunctional catalysts for LDH-supported noble-metal SACs applied in hybrid water electrolysis systems have also been reported. For example, Yu *et al.*[42] developed Pt single-atom sites (PtO_5) anchored NiCo-LDH supported by nickel foam (Pt_{SA}-NiCo-LDH/NF). In the electrocatalytic HER test, Pt_{SA}-NiCo-LDH/NF only required an overpotential of 63 mV to reach 100 mA cm^{-2}, lower than that of NiCo-LDH/NF (263 mV). DFT calculations indicated that the incorporation of Pt single-atom sites lowered the d-band center, and the HER barrier was reduced when two H atoms adsorb on these sites, resulting in improved HER performance. As for the anodic oxidation reaction, they substituted the OER by the glycerol oxidation reaction (GOR, 0.003V *vs.* RHE) while the anode reactant glycerol did not affect the HER performance. As expected, the potential required for Pt_{SA}-NiCo-LDH/NF at the current density of 100 mA cm^{-2} in GOR was 270 mV lower than OER, while high-value-added formic acid at the anode was formed. At the potential of 1.375 V, both the glycerol conversion (85%) and Faraday efficiency (88.7%) reached their highest levels. Moreover, the assembled hybrid water electrolysis system demonstrated superior performance to the overall water-splitting system.

The urea oxidation reaction (UOR) is fascinating due to the low thermodynamic equilibrium potential of 0.37 V *vs.* RHE, which is not only energy-efficient for hydrogen production but also provides a chance for pacificating urea-rich wastewater, demonstrating great promise for real-world applications. Sun *et al.*[102] anchored Rh single-atom sites (RhO_4) onto Ni-V hollow sites in NiV-LDH (Rh-NiV-LDH) to achieve bifunctional catalysts for UOR and HER. In the UOR process, a potential of 1.33 V *vs.* RHE sufficed to attain 10 mA cm^{-2}, lower than the potential needed for NiV-LDH (1.35 V *vs.* RHE), and marking a reduction of 200 mV compared to the potential required for the OER process. Rh-NiV-LDH also possessed outstanding HER activity, requiring only an overpotential of 12 mV to attain 10 mA cm^{-2}, lower than that of NiV-LDH (155 mV). DFT calculations indicated that Rh single-atom sites optimized the electronic structure of NiV-LDH, effectively lowering the reaction barriers in HER. Additionally, these sites optimized the adsorption and activation of urea, facilitating the desorption of CO* and NH*, significantly reducing the reaction barrier for UOR. Besides, Khalafallah *et al.*[103] dispersed Pt species as isolated atoms on NiCo-LDH (Pt_1/D-NiCo-LDH-24 SAC), also achieving a dual functional catalyst towards UOR (1.25 V *vs.* RHE to reach at 10 mA cm^{-2}) and HER (37 mV to reach at 10 mA cm^{-2}).

The theoretical potential of the hydrazine oxidation reaction (HzOR) is -0.33 V *vs.* RHE, which is 1.56 V lower than that of OER[104]. Additionally, the product of the HzOR is the inert gas N_2[36], rendering it highly safe. Wang *et al.*[105] found that Ru atoms in the form of RuO_4 coordination above the Fe sites of monolayer NiFe-LDH (Ru_1/mono-NiFe-1.6) are an efficient catalyst towards the HzOR. Ru_1/mono-NiFe-1.6 catalyst demonstrated a potential of just 1,260 mV at 10 mA cm^{-2}, significantly better than other catalysts including Ru_1/mono-NiFe-0.3 (1,301 mV), mono-NiFe (1,364 mV), and bulk-NiFe (1,394 mV). This catalyst also maintained its catalytic activity and stability over 600 cycles, with XPS signals of Ru, Fe, and Ni showing minimal changes after hydrazine electrooxidation, highlighting its durability. DFT calculations indicated that the addition of Ru increased the valance of Fe and stabilized the intermediates containing unpaired electrons ($*N_2H_3$ and $*N_2H$), leading to a transition in the rate-determining step (RDS) of HzOR from $*N_2H_2$ dehydrogenation to $*N_2H$ to the formation of $*N_2H_2$ specie, thereby reducing the energy barrier of the HzOR. To achieve a thorough understanding of the present research advancements, we have meticulously summarized the various applications of LDH-supported noble-metal SACs utilized for the anode reaction in hybrid water electrolysis [Table 2].

Thermal catalysis and photocatalysis

Thermal catalytic reactions are central to modern industrial chemical processes, involving the acceleration of chemical reactions through heating and the use of catalysts. In thermal catalysis, catalysts are typically employed to lower the activation energy of reactions, enabling them to proceed at lower temperatures or at

Table 2. LDH-supported noble-metal SACs for the anode reaction of hybrid water electrolysis

Noble metal	LDH type	Application	Performance (V)	Selectivity	Stability	Ref.
Pt (5.64 wt%)	NiCo-LDH	GOR	E_{100}: 1.298	88.7% (formate)	The current density is stable after 24 h	[42]
Ru (0.30 wt%)	NiFe-LDH	HMFOR	E_{onset}: 0.91	99.24% (FDCA)	Over 85% in FDCA selectivity after five cycles	[101]
Rh (6.59 wt%)	NiV-LDH	UOR	E_{100}: 1.33	-	~ 90% urea removal rate remained after three cycles	[102]
Pt (1.78 wt%)	NiCo-LDH	UOR	E_{10}: 1.25	-	No evident decay after 50 h test at different potentials	[103]
Rh (5.40 wt%)	NiFe-LDH	HzOR	E_{10}: 1.38	95% (N_2)	No evident decay after 1,000 CV cycles	[39]
Ru (1.60 wt%)	NiFe-LDH	HzOR	E_{10}: 1.26	98% (N_2)	No evident decay after 600 CV cycles	[105]

E_x: Potential (*vs.* RHE) required when the current density reaches x mA cm^{-2}; LDHs: layered double hydroxides; SACs: single-atom catalysts; HzOR: hydrazine oxidation reaction; GOR: glycerol oxidation reaction; HMFOR: 5-hydroxymethylfurfural oxidation; UOR: urea oxidation reaction; FDCA: 2,5-furan dicarboxylic acid; CV: cyclic voltammetry.

an increased rate[106]. Catalysts used in these processes can be either homogeneous (dissolved in the reaction medium) or heterogeneous (typically solid catalysts). Enhancing the activity and selectivity of industrial heterogeneous catalysts holds important significance from both profitable and environmental standpoints. The homogeneous distribution of active sites in SACs typically leads to high performance. However, until now, only a limited number of LDH-supported noble metal SACs have demonstrated remarkable performance in organic synthesis reactions [Table 3], including the hydrogenation of CO_2, selective benzyl alcohol oxidation, and anti-Markovnikov hydrosilylation of olefins. Given the crucial role of organic synthesis in the industry, there is a strong incentive to explore efficient LDH-supported noble metal SACs that can be applied in this field.

The hydrogenation of CO_2 to formic acid is vital for promoting sustainability, as it offers a renewable hydrogen storage solution while helping to reduce greenhouse gas emissions. Mori *et al.*[107] developed isolated Ru single-atom sites with an octahedral coordination geometry, consisting of one OH and two H_2O ligands, anchored to three O atoms derived from the original OH group on the surface of MgAl-LDH (Ru/LDH). Remarkably, this catalyst demonstrated excellent activity in the hydrogenation of CO_2 to formic acid. Ru/LDH achieved a high turnover number (TON) of 461 and a turnover frequency (TOF) of approximately 19 h^{-1}, with over 99% selectivity without forming methanol, outperforming other heterogeneous Ru catalysts. Ru/LDH demonstrated high catalytic performance even at low-pressure situations and could be reused no less than three times while maintaining 90% of its initial performance. The robustness and efficiency of this Ru/LDH are pivotal in advancing environmentally benign chemical processes. The ability of basic OH ligand triads at specific positions to donate electrons is essential for forming a highly active, electron-dense Ru center. Moreover, a clear connection is observed between the catalytic performance and the variable CO_2 adsorption capability surrounding the Ru center. By tweaking the composition and ratio of M^{2+}/M^{3+} in the LDH, the capacity for CO_2 adsorption around the Ru sites can be adjusted, with the optimal performance observed at a Mg^{2+}/Al^{3+} ratio of 5.

The selective aerobic oxidation reaction of benzyl alcohol to benzaldehyde represents a crucial transformation in organic synthesis, as it enables the efficient and environmentally friendly production of benzaldehyde, a valuable chemical intermediate with widespread industrial applications. Recently, our group[44] systematically investigated the microenvironment influence of NiFe-LDH-supported Ru SACs on the catalytic performance of benzyl alcohol oxidation [Figure 11A-C]. Three kinds of Ru SACs, Ru_1/LDH-V_{III} (RuO_6), Ru_1/LDH-V_{II} (RuO_6), and Ru_1/LDH (RuO_4) that are situated at trivalent metal

Table 3. LDH-supported noble-metal SACs for thermal catalysis and photocatalysis

Metal type	LDH type	Application	Selectivity	Stability	Ref.
Ru (1.10 wt%)	NiFe-LDH	Benzyl alcohol oxidation (thermal catalysis)	~ 100% (benzaldehyde)	Slightly decreased after five cycles	[44]
Pt (0.35 wt%)	CoFe-LDH	Alkene hydrosilylation (thermal catalysis)	99% (tri ethoxy(octyl)silane)	96.6% of original activity remained after ten cycles	[45]
Ru (0.36 wt%)	MgAl-LDH	Hydrogenation of CO_2 (thermal catalysis)	> 99% (formic acid)	90% of original activity remained after three cycles	[107]
Au (3.27 wt%)	MgAl-LDH	Benzene oxidation (photocatalysis)	99% (phenol)	No evident decay after five cycles	[41]

LDHs: Layered double hydroxides; SACs: single-atom catalysts.

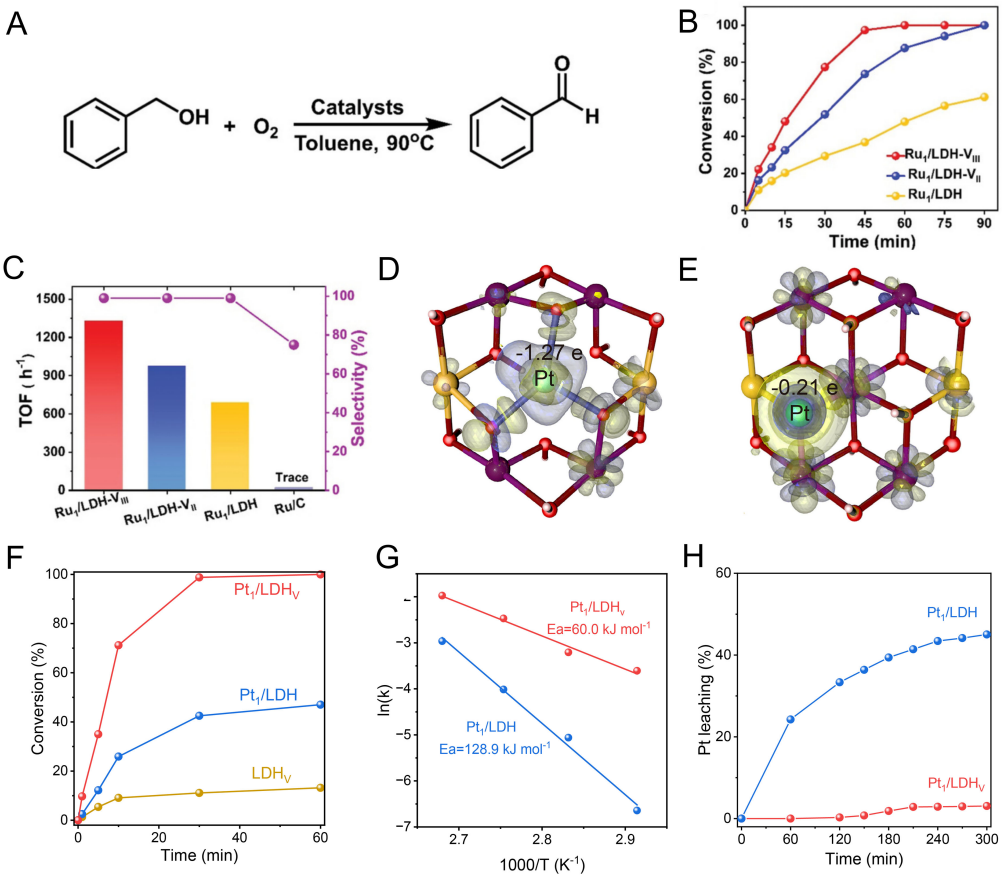

Figure 11. (A) The reaction for benzyl alcohol oxidation; (B) Plots of conversion versus time and (C) TOF value and selectivity of different catalysts[44]. Copyright 2022, Wiley-VCH; Simulated models and spatial electric field distributions of Pt_1/LDH_V (D) and Pt_1 /LDH (E); (F) Graphs of conversion over time for Pt-SACs and LDH supports; (G) Arrhenius plots on Pt_1/LDH_V and Pt_1/LDH; (H) Graphs of conversion over time for Pt-SACs prior to and following hot filtration[45]. Copyright 2024, Wiley-VCH. LDHs: Layered double hydroxides; SACs: single-atom catalysts; TOF: turnover frequency.

vacancies, divalent metal vacancies, and the surface of NiFe-LDH, respectively were synthesized and compared. Among them, $Ru_1/LDH\text{-}V_{III}$ achieved 99% conversion of the benzaldehyde after one hour, higher than that of $Ru_1/LDH\text{-}V_{II}$ (87.7%) and Ru_1/LDH (47.9%), while the selectivity of them was all 100%. TOF values were 1,331 h^{-1}, 976 h^{-1}, and 659 h^{-1} for $Ru_1/LDH\text{-}V_{III}$, $Ru_1/LDH\text{-}V_{II}$, and Ru_1/LDH, respectively, much higher than that of commercial Ru/C. Theoretical calculations showed that the desorption of benzaldehyde was the RDS for benzyl alcohol oxidation, and the Ru sites in $Ru_1/LDH\text{-}V_{III}$ required lower benzaldehyde

desorption energy (1.20 eV) than Ru_1/LDH-V_{II} (1.33 eV) and Ru_1/LDH (1.91 eV). Therefore, the Ru sites in Ru_1/LDH-V_{III} possessed the highest activity in selective benzyl alcohol oxidation. This work evidenced that the microenvironment of noble-metal single-atoms on LDH laminates is crucial for their catalytic activity.

The process of alkene hydrosilylation, involving the adding of Si-H to the C=C, is a pivotal industrial reaction widely used in the production of functional organosilicon compounds vital to various fields such as materials science, iatrochemistry, and medicinal chemistry, making it one of the most important large-scale reactions. We recently prepared an efficient catalyst for this reaction by anchoring Pt single-atom sites onto the divalent cation vacancies of CoFe-LDH (Pt_1/LDH_V) in the form of PtO_3 coordination [Figure 11D-H][45]. The Pt_1/LDH_V exhibited efficient catalytic activity in the alkene hydrosilylation reaction of 1-octene and triethoxysilane, achieving a high conversion rate of ≈ 99%, and only the anti-Markovnikov addition product was detected. Additionally, the catalytic performance of Pt_1/LDH_V (with a TOF value of 130,000 h^{-1}) surpassed that of other alternative catalysts and most reported noble-metal SACs. Notably, this Pt_1/LDH_V catalyst demonstrated remarkable stability and activity retention after ten reaction cycles, with catalytic efficiency loss lower than most reported noble metal SACs. The superior performance and stability of Pt_1/LDH_V in anti-Markovnikov alkene hydrosilylation stem from the enhanced electron-metal support interaction that stabilizes Pt atoms via surrounding oxygen atoms. This stabilization facilitates electron transfer to Si-C bonds, accelerating RDS, and promoting product detachment, thereby ensuring high catalytic activity.

Besides the above thermal catalytic organic synthesis, the LDH-supported noble metal SACs also demonstrated potential in selective organic synthesis powered by light. Shen *et al.*[41] reported that Au_1-MgAl-LDH with the individual Au atoms (AuO_4) located on the top of Al^{3+} exhibited excellent photocatalytic performance for benzene oxidation to phenol. This material exhibited excellent selectivity for phenol (> 99%) without other over-oxidative products, while the Au nanoparticle counterpart (Au-NP-MgAl-LDH) showed a ≈ 99% selectivity for aliphatic acid, highlighting the merits of forming Au SACs. The combination of in situ XAFS and DFT calculations revealed that the AuO_3 intermediate serves as the active site for benzene oxidation, where benzene is activated through the formation of a single Au-C bond, leading to phenol production. To gain a comprehensive understanding of the current research, we have summarized the current application of LDH-supported noble-metal SACs in thermal catalysis and, photocatalysis, as listed in Table 3.

Enzyme-like applications

The biosafety of LDH-supported noble-metal SACs confers them with potential for enzyme-like applications. Recently, our group[43] first found that MgAl-LDH with Ru single-atom sites (RuO_3) on the surface (Ru_1/LDH) can serve as an artificial nanoenzyme to achieve efficient scavenging of reactive radicals. Ru_1/LDH demonstrated excellent peroxidase (POD)-like catalytic performance, exhibiting 20 times higher catalytic efficiency (k_{cat}/K_m = 1.69 × 10^4 S^{-1} M^{-1}) than Ru NCs/LDH (Ru nanoparticles anchored on MgAl-LDH) in the conversion of H_2O_2 to O* under acidic conditions. This can be ascribed to the heterolytic dissociation mechanism of H_2O_2 at the individual Ru sites, which need less free energy (0.43 eV) for dissociation compared to the homolytic dissociation route on Ru nanoparticles (0.63 eV). The Ru_1/LDH demonstrated outstanding capacity to scavenge various free radicals, including superoxide anion radical, 2, 2-diphenyl-1-picrylhydrazyl radical (DPPH•), •OH, and NO•. The intracellular antioxidative activities of Ru_1/LDH resulted in an efficient elimination of approximately 83% of ROS [Figure 12A and B]. Remarkably, even after a prolonged duration of 48 h, Ru_1/LDH exhibited exceptional stability by scavenging up to 97% of ROS [Figure 12C and D].

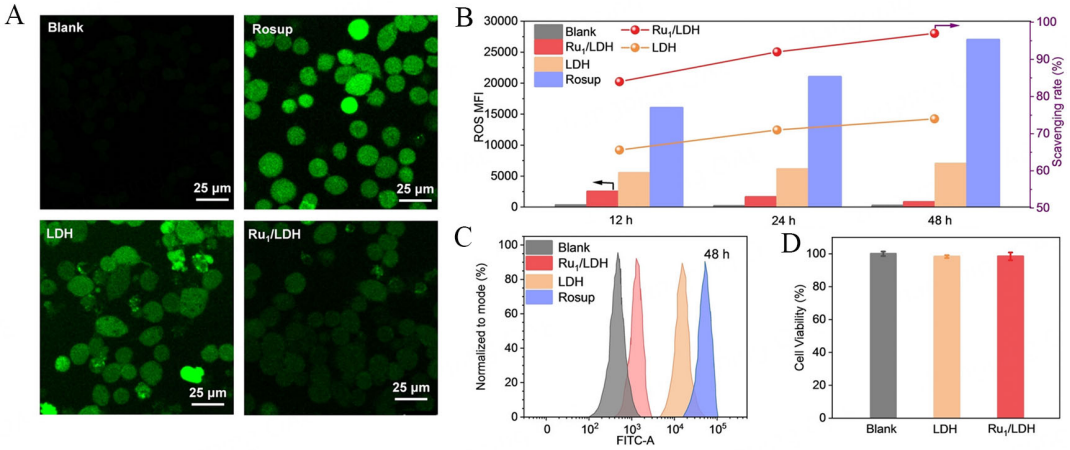

Figure 12. (A) Assessment of ROS scavenging capacity of Ru_1/LDH and LDH using fluorescence microscopy; (B) Time-dependent intracellular antioxidant activities and average intracellular fluorescence intensity of Ru_1/LDH and LDH; (C) Normalized flow cytometry analysis of intracellular ROS after 48 h of Rosup stimulation with different enzymes; (D) Cell viability following 12 h incubation with LDH and Ru_1/LDH[43]. Copyright 2023, Wiley-VCH. LDHs: Layered double hydroxides; ROS: reactive oxygen species.

The LDH-supported noble-metal SACs also exhibited excellent activity in the anti-bacterial field. Zhou *et al.*[108] developed a Ru SAC (RuO_4) supported on the surface of NiFe-LDH (Ru/NiFe-LDH) in the activation of peroxymonosulfate (PMS) to deactivate Escherichia coli (E. coli). With the combined action of low concentrations of Ru/NiFe-LDH (40 mg/L) and PMS (5 mg/L), full inactivation of 7 log E. coli was achieved in 90 seconds. The Ru/NiFe-LDH activated PMS, generating key reactive oxygen species, notably electrophilic $^1O_2$, serving as the main active species responsible for the rapid deactivation of E. coli.

CONCLUSION AND PERSPECTIVE

In summary, LDH-supported noble-metal SACs have garnered significant attention from researchers and have undergone rapid developments recently. LDHs exhibit an adjustable structure, offering multi-selectivity in anchoring positions of noble-metal single-atom sites. This, coupled with the strong electronic interactions between LDH supports and noble-metal atoms, endows LDH-supported noble-metal SACs with remarkable flexibility in structural design. Such flexibility illuminates promising application potential for LDH-supported noble-metal SACs across various heterogeneous catalysis domains, deserving special attention. In this review, we focused on the strategies employed for synthesis and the applications of LDH-supported noble-metal SACs. Despite significant advancements made so far, there are still great opportunities and huge challenges in the future development of this area.

The precise tuning of noble-metal single-atom sites

Precise tuning is essential for optimizing the catalytic properties of noble-metal SACs. Due to the unique and adjustable structure of LDHs, noble-metal single-atom sites tend to stabilize at the position with the lowest formation energy, making directional anchoring on LDHs possible. However, most of the reported LDH-supported SACs mainly focus on LDH with laminates composed of two kinds of non-noble metals. Introducing a third or more non-noble metals into LDH laminates may further regulate the electronic structure of the laminates, thereby obtaining stronger directional anchoring ability of noble-metal atoms. In addition, the modification of axial ligands and the coordination number regulation of noble-metal atoms also face significant challenges. The modulation of the microenvironments of noble-metal single-atom sites can further adjust the dynamic changes of active sites and the adsorption behavior of intermediates during the catalytic process, thereby imparting distinct catalytic stability, activity, and selectivity to the catalysts. Precise tuning allows for a deeper understanding of catalytic mechanisms, which paves the way for

designing catalysts with improved efficiency and selectivity. Therefore, despite challenges, precise tuning of LDH-supported SACs holds promise for catalytic advancements.

The high loading of noble-metal single-atom sites

Achieving the high loading of noble-metal single-atom sites is tricky due to the high surface energy. The strong co-catalytic metal-support interactions between LDHs and noble-metal atoms provide feasibility for achieving high loading of noble-metal single-atom sites. However, most of the reported LDH-supported SACs currently have low noble-metal loading (< 3 wt%). Therefore, developing specific synthesis strategies to increase the loading of noble-metal single-atom sites is the focus of future research work. Improving the loading of noble-metal single atoms is the key to optimizing the catalytic performance of LDH-supported noble-metal SACs.

The role of interlayer anions in LDHs

The interlayer anions, such as CO_3^{2-}, Cl^-, NO_3^-, SO_4^{2-}, OH^-, PO_4^{3-}, CH_3COO^-, *etc.*, influence the overall chemical environment of LDHs, thereby shaping the properties and behavior of LDH-supported catalysts. The introduction of a variety of interlayer anions has not only enriched the catalog of LDH-based catalysts but also offered enhanced structural flexibility for fine-tuning their performance. Currently, understanding how interlayer anions alter the characteristics of LDHs remains a focal point of scientific inquiry. However, despite the recognized significance of interlayer anions, existing research on LDH-supported noble-metal SACs has predominantly focused on CO_3^{2-} intercalation, neglecting the potential contributions of other interlayer anions. The exploration of diverse interlayer anions promises to endow LDH-supported noble-metal SACs with greater structural variety and broader applicability. Therefore, it is imperative to delve into the fundamental mechanisms that underlie the interplay between interlayer anions and catalytic performance. This understanding is pivotal for advancing the design and optimization of LDH-supported noble-metal SACs, unlocking their full catalytic potential.

The stability of LDH-supported noble-metal SACs

The high surface energy of single-atom sites significantly enhances their mobility on the support. During catalysis, when reactants adsorb onto these single-atom sites, the interaction between single-atom sites and the support weakens, leading to their migration and aggregation into clusters or particles, or even detachment from the support. This issue is particularly pronounced under harsh operating conditions, where stability is further compromised. Although most reported LDH-supported noble-metal SACs demonstrate good stability, maintaining high activity after several hundred hours or multiple cycles, they remain distant from industrial-scale application. Enhancing the interaction between noble-metal single-atom sites and the LDH support, such as through modifying the LDH support or adjusting the microenvironment of the noble-metal single-atom sites, can help prevent them from moving or detaching during reactions, thus improving stability. Additionally, employing spatial confinement strategies to limit the movement of noble-metal single-atom sites and reduce the possibility of their aggregation is another effective strategy. Future research focusing on further enhancing the stability of LDH-supported noble-metal SACs will be crucial for their transition to large-scale industrial applications.

The development of DACs/MACs

As the field of SACs progresses, their inherent limitations have become increasingly apparent to researchers. For instance, SACs, which only feature one metal center, face difficulties in the reactions based on multi-site adsorptions that are common in numerous catalytic reactions. This constraint poses substantial challenges to the widespread exploration and application of SACs across various catalytic domains. In light of these restrictions, the advent of DACs and MACs, evolving from SACs, has generated significant excitement among the scientific community. Previous investigations have revealed that interactions between two or

more metal single-atom sites, including synergistic effects, distance-enhancement effects (also known as geometric effects), and electronic effects, can effectively address some of the limitations encountered in SAC applications. Furthermore, the steric hindrance effect among different atoms serves to efficiently hinder the aggregation of identical metal atoms, thereby enabling DACs and MACs to accommodate higher metal atom loadings compared to SACs. It is worth noting that, to date, there have been no reports on LDH-supported noble-metal DACs or MACs. The development of such catalysts holds immense importance in overcoming the current challenges faced by SACs and unlocking new possibilities in the field of catalysis.

The application of in-situ characterization

In the aforementioned research, the anchoring form and coordination environment of noble-metal single-atom sites are usually determined by AC-STEM and XAS techniques. The above information obtained is used to construct theoretical models for DFT, revealing the intrinsic mechanisms between the microenvironment of noble-metal single-atom sites and catalytic performance. However, the electronic structure and coordination of noble-metal single-atom sites tend to change during electrochemical processes. The inability of these characterizations to capture such changes in the working state leads to differences between DFT computational results and the actual reaction mechanism. Therefore, employing advanced in-situ characterization techniques, such as in-situ XAS and single-atom electron spectroscopy, to further capture the changes in the electronic structure, the coordination environment of noble-metal single-atom sites, and the co-catalytic metal-support interactions during catalysis, can contribute to a more accurate understanding of the catalytic mechanism of LDH-supported noble-metal SACs.

The establishment of advanced intelligent synthesis platforms

The application exploration and performance optimization of SACs is mainly based on a terrific amount of repetitive experiments. However, with the rapid development of artificial intelligence (AI) and robot technology, researchers are expected to break free from the above inefficient and labor-intensive process. Researchers can use AI combined with DFT to establish predictive catalyst models and achieve rapid reaction parameter screening and catalyst preparation *via* high-throughput screening and laboratory robot technology. Notably, the highly ordered and adjustable crystal structure and the relatively facile synthesis step of LDH-supported noble-metal SACs provide favorable conditions for the realization of intelligent synthesis. The establishment of advanced intelligent synthesis platforms can significantly improve the work efficiency of researchers, allowing them to have more time to focus on more valuable work.

Further exploration in application fields

LDH-supported noble-metal SACs hold immense potential across various fields, including electrocatalysis, thermal catalysis, photocatalysis, energy storage, and medical treatment. However, current research on these materials primarily focuses on a limited scope within electrocatalysis, specifically in water splitting and hybrid water electrolysis. Notably, LDH-supported materials and noble-metal-based catalysts have already demonstrated diverse applications in other electrocatalytic reactions, such as carbon dioxide, nitrate, and nitrogen reduction reactions. Moreover, there is a noticeable scarcity of reports on the use of LDH-supported noble-metal SACs in thermal catalysis and medical treatment compared to their use in electrocatalysis. Given the versatility and potential of LDH-supported noble-metal SACs, there is a pressing need for more researchers to explore their applications in other catalytic fields. This underserved area of research offers rich opportunities for discovery and innovation. Therefore, we strongly encourage further exploration and investigation into the diverse potential applications of LDH-supported noble-metal SACs.

Large-scale industrial production

LDHs have achieved large-scale industrial production and application due to their facile synthesis, cost-effectiveness, and environmental compatibility. As a branch of LDH-based catalysts, LDH-supported noble-metal SACs inherit the above advantages, while the introduction of noble-metal single-atom sites has further improved their performance and expanded their application fields. However, most reported catalysts belong to laboratory-scale synthesis, far from large-scale industrial production. Developing a large-scale synthesis strategy for LDH-supported noble-metal SACs is of great significance in promoting their industrialization process.

DECLARATIONS

Authors' contributions

Made the literature review and drafted the original version: Liu, D.
Literature survey and organization: Liu, D.; Zhang, T.; Gu, X.; Yang, X.
Revised the manuscript: Liu, D.; Zhang, T.; Han, A.; Liu, J.
Conceived and supervised the project: Han, A.; Liu, J.

Availability of data and materials

Not applicable.

Financial support and sponsorship

This work was financially supported by the Beijing Natural Science Foundation (Z240027), the National Natural Science Foundation of China (NSFC), and the Fundamental Research Funds for the Central Universities.

Conflicts of interest

All authors declared that there are no conflicts of interest.

Ethical approval and consent to participate

Not applicable.

Consent for publication

Not applicable.

REFERENCES

1. Liang, X.; Fu, N.; Yao, S.; Li, Z.; Li, Y. The progress and outlook of metal single-atom-site catalysis. *J. Am. Chem. Soc.* **2022**, *144*, 18155-74. DOI
2. Wang, W.; Zeng, C.; Tsubaki, N. Recent advancements and perspectives of the CO_2 hydrogenation reaction. *Green. Carbon.* **2023**, *1*, 133-45. DOI
3. Yang, Q.; Liu, W.; Wang, B.; et al. Regulating the spatial distribution of metal nanoparticles within metal-organic frameworks to enhance catalytic efficiency. *Nat. Commun.* **2017**, *8*, 14429. DOI PubMed PMC
4. Liu, W.; Huang, J.; Yang, Q.; et al. Multi-shelled hollow metal-organic frameworks. *Angew. Chem. Int. Ed.* **2017**, *56*, 5512-6. DOI
5. Meng, G.; Sun, W.; Mon, A. A.; et al. Strain regulation to optimize the acidic water oxidation performance of atomic-layer IrO_x. *Adv. Mater.* **2019**, *31*, e1903616. DOI
6. Jin, J.; Fang, Y.; Zhang, T.; Han, A.; Wang, B.; Liu, J. Ultrasmall Ag nanoclusters anchored on NiCo-layered double hydroxide nanoarray for efficient electrooxidation of 5-hydroxymethylfurfural. *Sci. China. Mater.* **2022**, *65*, 2704-10. DOI
7. Yang, G.; Wang, D.; Wang, Y.; et al. Modulating the primary and secondary coordination spheres of single Ni(II) sites in metal-organic frameworks for boosting photocatalysis. *J. Am. Chem. Soc.* **2024**, *146*, 10798-805. DOI
8. Shi, Z.; Zhang, X.; Lin, X.; et al. Phase-dependent growth of Pt on MoS_2 for highly efficient H_2 evolution. *Nature* **2023**, *621*, 300-5.

DOI

9. Wang, Q.; Wang, H.; Cao, H.; et al. Atomic metal-non-metal catalytic pair drives efficient hydrogen oxidation catalysis in fuel cells. *Nat. Catal.* **2023**, *6*, 916-26. DOI
10. Li, Y.; Sun, Y.; Qin, Y.; et al. Recent advances on water-splitting electrocatalysis mediated by noble-metal-based nanostructured materials. *Adv. Energy. Mater.* **2020**, *10*, 1903120. DOI
11. Li, X.; Mitchell, S.; Fang, Y.; Li, J.; Perez-Ramirez, J.; Lu, J. Advances in heterogeneous single-cluster catalysis. *Nat. Rev. Chem.* **2023**, *7*, 754-67. DOI
12. Qiao, B.; Wang, A.; Yang, X.; et al. Single-atom catalysis of CO oxidation using Pt_1/FeO*x*. *Nat. Chem.* **2011**, *3*, 634-41. DOI
13. Li, X.; Rong, H.; Zhang, J.; Wang, D.; Li, Y. Modulating the local coordination environment of single-atom catalysts for enhanced catalytic performance. *Nano. Res.* **2020**, *13*, 1842-55. DOI
14. Zhou, A.; Wang, D.; Li, Y. Hollow microstructural regulation of single-atom catalysts for optimized electrocatalytic performance. *Microstructures* **2021**,. DOI
15. Liang, C.; Han, X.; Zhang, T.; et al. Cu nanoclusters accelerate the rate-determining step of oxygen reduction on Fe-N-C in all pH range. *Adv. Energy. Mater.* **2024**, *14*, 2303935. DOI
16. Han, A.; Wang, B.; Kumar, A.; et al. Recent advances for MOF-derived carbon-supported single-atom catalysts. *Small. Methods.* **2019**, *3*, 1800471. DOI
17. Zhang, N.; Zhang, X.; Tao, L.; et al. Silver single-atom catalyst for efficient electrochemical CO_2 reduction synthesized from thermal transformation and surface reconstruction. *Angew. Chem. Int. Ed.* **2021**, *60*, 6170-6. DOI
18. Zhang, N.; Yan, H.; Li, L.; et al. Use of rare earth elements in single-atom site catalysis: a critical review - commemorating the 100th anniversary of the birth of Academician Guangxian Xu. *J. Rare. Earths.* **2021**, *39*, 233-42. DOI
19. Rocha, G. F. S. R.; da, S. M. A. R.; Rogolino, A.; et al. Carbon nitride based materials: more than just a support for single-atom catalysis. *Chem. Soc. Rev.* **2023**, *52*, 4878-932. DOI
20. Ma, Z.; Zhang, T.; Lin, L.; Han, A.; Liu, J. Ni single-atom arrays as self-supported electrocatalysts for CO_2RR. *AIChE. J.* **2023**, *69*, e18161. DOI
21. Han, X.; Zhang, T.; Wang, X.; et al. Hollow mesoporous atomically dispersed metal-nitrogen-carbon catalysts with enhanced diffusion for catalysis involving larger molecules. *Nat. Commun.* **2022**, *13*, 2900. DOI PubMed PMC
22. Zhang, T.; Han, X.; Yang, H.; et al. Atomically dispersed Nickel(I) on an alloy-encapsulated nitrogen-doped carbon nanotube array for high-performance electrochemical CO_2 reduction reaction. *Angew. Chem. Int. Ed.* **2020**, *59*, 12055-61. DOI
23. Zhao, Y.; Tian, Z.; Wang, W.; Deng, X.; Tseng, J.; Wang, G. Size-dependent activity of Fe-N-doped mesoporous carbon nanoparticles towards oxygen reduction reaction. *Green. Carbon.* **2024**, *2*, 221-30. DOI
24. Zhao, C. X.; Li, B. Q.; Liu, J. N.; Zhang, Q. Intrinsic electrocatalytic activity regulation of M-N-C single-atom catalysts for the oxygen reduction reaction. *Angew. Chem. Int. Ed.* **2021**, *60*, 4448-63. DOI PubMed
25. Iemhoff, A.; Vennewald, M.; Palkovits, R. Single-atom catalysts on covalent triazine frameworks: at the crossroad between homogeneous and heterogeneous catalysis. *Angew. Chem. Int. Ed.* **2023**, *62*, e202212015. DOI PubMed PMC
26. Zhao, W.; Shen, J.; Xu, X.; et al. Functional catalysts for polysulfide conversion in Li-S batteries: from micro/nanoscale to single atom. *Rare. Met.* **2022**, *41*, 1080-100. DOI
27. Zhang, T.; Wang, F.; Yang, C.; et al. Boosting ORR performance by single atomic divacancy Zn-N_3C-C_8 sites on ultrathin N-doped carbon nanosheets. *Chem. Catal.* **2022**, *2*, 836-52. DOI
28. Han, X.; Zhang, T.; Chen, W.; et al. Mn-N_4 oxygen reduction electrocatalyst: operando investigation of active sites and high performance in zinc-air battery. *Adv. Energy. Mater.* **2021**, *11*, 2002753. DOI
29. Wang, C.; Humayun, M.; Debecker, D. P.; Wu, Y. Electrocatalytic water oxidation with layered double hydroxides confining single atoms. *Coord. Chemistry. Rev.* **2023**, *478*, 214973. DOI
30. Zhou, D.; Li, P.; Lin, X.; et al. Layered double hydroxide-based electrocatalysts for the oxygen evolution reaction: identification and tailoring of active sites, and superaerophobic nanoarray electrode assembly. *Chem. Soc. Rev.* **2021**, *50*, 8790-817. DOI
31. Wang, Y.; Zhang, M.; Liu, Y.; et al. Recent advances on transition-metal-based layered double hydroxides nanosheets for electrocatalytic energy conversion. *Adv. Sci.* **2023**, *10*, e2207519. DOI
32. Fan, G.; Li, F.; Evans, D. G.; Duan, X. Catalytic applications of layered double hydroxides: recent advances and perspectives. *Chem. Soc. Rev.* **2014**, *43*, 7040-66. DOI PubMed
33. Long, X.; Wang, Z.; Xiao, S.; An, Y.; Yang, S. Transition metal based layered double hydroxides tailored for energy conversion and storage. *Mater. Today.* **2016**, *19*, 213-26. DOI
34. Lang, R.; Du, X.; Huang, Y.; et al. Single-atom catalysts based on the metal-oxide interaction. *Chem. Rev.* **2020**, *120*, 11986-2043. DOI
35. Shi, Q.; Cheng, M.; Liu, Y.; et al. In-situ generated MOFs with supportive LDH substrates and their derivatives for photo-electrocatalytic energy production and electrochemical devices: insights into synthesis, function, performance and mechanism. *Coord. Chem. Rev.* **2024**, *499*, 215500. DOI
36. Hu, T.; Gu, Z.; Williams, G. R.; et al. Layered double hydroxide-based nanomaterials for biomedical applications. *Chem. Soc. Rev.* **2022**, *51*, 6126-76. DOI
37. Jiang, S.; Zhang, M.; Xu, C.; et al. Recent developments in nickel-based layered double hydroxides for photo(-/)electrocatalytic water oxidation. *ACS. Nano.* **2024**, *18*, 16413-49. DOI

38. Yan, H.; Lu, J.; Wei, M.; et al. Theoretical study of the hexahydrated metal cations for the understanding of their template effects in the construction of layered double hydroxides. *J. Mol. Struct:. THEOCHEM.* **2008**, *866*, 34-45. DOI
39. Liu, G.; Wang, Z.; Shen, T.; Zheng, X.; Zhao, Y.; Song, Y. F. Atomically dispersed Rh-doped NiFe layered double hydroxides: precise location of Rh and promoting hydrazine electrooxidation properties. *Nanoscale* **2021**, *13*, 1869-74. DOI
40. Sun, H.; Tung, C. W.; Qiu, Y.; et al. Atomic metal-support interaction enables reconstruction-free dual-site electrocatalyst. *J. Am. Chem. Soc.* **2022**, *144*, 1174-86. DOI
41. Shen, T.; Song, Z.; Li, J.; et al. Enabling specific benzene oxidation by tuning the adsorption behavior on Au loaded MgAl layered double hydroxides. *Small* **2023**, *19*, e2303420. DOI
42. Yu, H.; Wang, W.; Mao, Q.; et al. Pt single atom captured by oxygen vacancy-rich NiCo layered double hydroxides for coupling hydrogen evolution with selective oxidation of glycerol to formate. *Appl. Catal. B:. Environ.* **2023**, *330*, 122617. DOI
43. Wang, B.; Fang, Y.; Han, X.; et al. Atomization-induced high intrinsic activity of a biocompatible MgAl-LDH supported Ru single-atom nanozyme for efficient radicals scavenging. *Angew. Chem. Int. Ed.* **2023**, *62*, e202307133. DOI
44. Jin, J.; Han, X.; Fang, Y.; et al. Microenvironment engineering of Ru single-atom catalysts by regulating the cation vacancies in NiFe-layered double hydroxides. *Adv. Funct. Mater.* **2022**, *32*, 2109218. DOI
45. Zhang, T.; Yang, X.; Jin, J.; et al. Modulating the electronic metal-support interactions to anti-leaching Pt single atoms for efficient hydrosilylation. *Adv. Mater.* **2024**, *36*, e2304144. DOI
46. Zhang, T.; Jin, J.; Chen, J.; et al. Pinpointing the axial ligand effect on platinum single-atom-catalyst towards efficient alkaline hydrogen evolution reaction. *Nat. Commun.* **2022**, *13*, 6875. DOI PubMed PMC
47. Li, P.; Wang, M.; Duan, X.; et al. Boosting oxygen evolution of single-atomic ruthenium through electronic coupling with cobalt-iron layered double hydroxides. *Nat. Commun.* **2019**, *10*, 1711. DOI PubMed PMC
48. Hu, Y.; Shen, T.; Song, Z.; et al. Atomic modulation of single dispersed Ir species on self-supported NiFe layered double hydroxides for efficient electrocatalytic overall water splitting. *ACS. Catal.* **2023**, *13*, 11195-203. DOI
49. Chen, W.; Wu, B.; Wang, Y.; et al. Deciphering the alternating synergy between interlayer Pt single-atom and NiFe layered double hydroxide for overall water splitting. *Energy. Environ. Sci.* **2021**, *14*, 6428-40. DOI
50. Cao, X.; Qiao, Y.; Jia, M.; He, P.; Zhou, H. Ion-exchange: a promising strategy to design Li-rich and Li-excess layered cathode materials for Li-ion batteries. *Adv. Energy. Mater.* **2022**, *12*, 2003972. DOI
51. Chen, S.; Tao, R.; Guo, C.; et al. A new trick for an old technology: ion exchange syntheses of advanced energy storage and conversion nanomaterials. *Energy. Storage. Maters.* **2021**, *41*, 758-90. DOI
52. Mu, X.; Gu, X.; Dai, S.; et al. Breaking the symmetry of single-atom catalysts enables an extremely low energy barrier and high stability for large-current-density water splitting. *Energy. Environ. Sci.* **2022**, *15*, 4048-57. DOI
53. Chung, D. Y.; Lopes, P. P.; Farinazzo, B. D. M. P.; et al. Dynamic stability of active sites in hydr(oxy)oxides for the oxygen evolution reaction. *Nat. Energy.* **2020**, *5*, 222-30. DOI
54. Lin, X.; Wang, Z.; Cao, S.; et al. Bioinspired trimesic acid anchored electrocatalysts with unique static and dynamic compatibility for enhanced water oxidation. *Nat. Commun.* **2023**, *14*, 6714. DOI PubMed PMC
55. Kuai, C.; Xu, Z.; Xi, C.; et al. Phase segregation reversibility in mixed-metal hydroxide water oxidation catalysts. *Nat. Catal.* **2020**, *3*, 743-53. DOI
56. He, W.; Zhang, R.; Liu, H.; et al. Atomically dispersed silver atoms embedded in NiCo layer double hydroxide boost oxygen evolution reaction. *Small* **2023**, *19*, e2301610. DOI
57. Wang, F.; Zou, P.; Zhang, Y.; et al. Activating lattice oxygen in high-entropy LDH for robust and durable water oxidation. *Nat. Commun.* **2023**, *14*, 6019. DOI PubMed PMC
58. Ling, T.; Jaroniec, M.; Qiao, S. Z. Recent progress in engineering the atomic and electronic structure of electrocatalysts via cation exchange reactions. *Adv. Mater.* **2020**, *32*, e2001866. DOI PubMed
59. Nandan, R.; Devi, H. R.; Kumar, R.; Singh, A. K.; Srivastava, C.; Nanda, K. K. Inner sphere electron transfer promotion on homogeneously dispersed Fe-N*x* centers for energy-efficient oxygen reduction reaction. *ACS. Appl. Mater. Interfaces.* **2020**, *12*, 36026-39. DOI
60. Chen, Y.; Lin, J.; Jia, B.; Wang, X.; Jiang, S.; Ma, T. Isolating single and few atoms for enhanced catalysis. *Adv. Mater.* **2022**, *34*, e2201796. DOI
61. Li, X.; Liu, L.; Ren, X.; Gao, J.; Huang, Y.; Liu, B. Microenvironment modulation of single-atom catalysts and their roles in electrochemical energy conversion. *Sci. Adv.* **2020**, 6. DOI PubMed PMC
62. Han, B.; Luo, Y.; Lin, Y.; et al. Microenvironment engineering of single-atom catalysts for persulfate-based advanced oxidation processes. *Chem. Eng. J.* **2022**, *447*, 137551. DOI
63. Lai, W.; Miao, Z.; Wang, Y.; Wang, J.; Chou, S. Atomic-local environments of single-atom catalysts: synthesis, electronic structure, and activity. *Adv. Energy. Mater.* **2019**, *9*, 1900722. DOI
64. Wang, L.; Ma, M.; Zhang, C.; et al. Manipulating the microenvironment of single atoms by switching support crystallinity for industrial hydrogen evolution. *Angew. Chem. Int. Ed.* **2024**, *63*, e202317220. DOI
65. Yang, P. P.; Gao, M. R. Enrichment of reactants and intermediates for electrocatalytic CO_2 reduction. *Chem. Soc. Rev.* **2023**, *52*, 4343-80. DOI PubMed
66. Han, S. G.; Ma, D. D.; Zhu, Q. L. Atomically structural regulations of carbon-based single-atom catalysts for electrochemical CO_2 reduction. *Small. Methods.* **2021**, *5*, e2100102. DOI PubMed

67. Li, J.; Zhang, L.; Doyle□davis, K.; Li, R.; Sun, X. Recent advances and strategies in the stabilization of single-atom catalysts for electrochemical applications. *Carbon. Energy.* **2020**, *2*, 488-520. DOI
68. Gloag, L.; Somerville, S. V.; Gooding, J. J.; Tilley, R. D. Co-catalytic metal-support interactions in single-atom electrocatalysts. *Nat. Rev. Mater.* **2024**, *9*, 173-89. DOI
69. Qi, K.; Chhowalla, M.; Voiry, D. Single atom is not alone: metal-support interactions in single-atom catalysis. *Mater. Today.* **2020**, *40*, 173-92. DOI
70. Zhang, L.; Zhao, X.; Yuan, Z.; Wu, M.; Zhou, H. Oxygen defect-stabilized heterogeneous single atom catalysts: preparation, properties and catalytic application. *J. Mater. Chem. A.* **2021**, *9*, 3855-79. DOI
71. Zhang, Y.; Guo, L.; Tao, L.; Lu, Y.; Wang, S. Defect-based single-atom electrocatalysts. *Small. Methods.* **2019**, *3*, 1800406. DOI
72. Yang, J.; An, L.; Wang, S.; et al. Defects engineering of layered double hydroxide-based electrocatalyst for water splitting. *Chin. J. Catal.* **2023**, *55*, 116-36. DOI
73. Xie, Q.; Cai, Z.; Li, P.; et al. Layered double hydroxides with atomic-scale defects for superior electrocatalysis. *Nano. Res.* **2018**, *11*, 4524-34. DOI
74. Zhai, P.; Xia, M.; Wu, Y.; et al. Engineering single-atomic ruthenium catalytic sites on defective nickel-iron layered double hydroxide for overall water splitting. *Nat. Commun.* **2021**, *12*, 4587. DOI PubMed PMC
75. Fan, B.; Wang, W.; Liu, Z.; Guo, J.; Yuan, H.; Tan, Y. Recent progress in single atomic catalysts for electrochemical N_2 fixation. *Microstructures* **2024**, *4*, 2024025. DOI
76. Liu, X.; Liu, Y.; Yang, W.; Feng, X.; Wang, B. Controlled modification of axial coordination for transition-metal single-atom electrocatalyst. *Chem. Eur. J.* **2022**, *28*, e202201471. DOI
77. Zhang, L.; Jin, N.; Yang, Y.; et al. Advances on axial coordination design of single-atom catalysts for energy electrocatalysis: a review. *Nano-Micro. Lett.* **2023**, *15*, 228. DOI PubMed PMC
78. Duan, X.; Sha, Q.; Li, P.; et al. Dynamic chloride ion adsorption on single iridium atom boosts seawater oxidation catalysis. *Nat. Commun.* **2024**, *15*, 1973. DOI PubMed PMC
79. Duan, X.; Li, P.; Zhou, D.; et al. Stabilizing single-atomic ruthenium by ferrous ion doped NiFe-LDH towards highly efficient and sustained water oxidation. *Chem. Eng. J.* **2022**, *446*, 136962. DOI
80. Roth-zawadzki, A. M.; Nielsen, A. J.; Tankard, R. E.; Kibsgaard, J. Dual and triple atom electrocatalysts for energy conversion (CO_2 RR, NRR, ORR, OER, and HER): synthesis, characterization, and activity evaluation. *ACS. Catal.* **2024**, *14*, 1121-45. DOI
81. Wang, Y.; Mao, J.; Meng, X.; Yu, L.; Deng, D.; Bao, X. Catalysis with two-dimensional materials confining single atoms: concept, design, and applications. *Chem. Rev.* **2019**, *119*, 1806-54. DOI
82. Zhang, W.; Zhao, Y.; Huang, W.; Huang, T.; Wu, B. Coordination environment manipulation of single atom catalysts: regulation strategies, characterization techniques and applications. *Coord. Chem. Rev.* **2024**, *515*, 215952. DOI
83. Finzel, J.; Sanroman, G. K. M.; Hoffman, A. S.; Resasco, J.; Christopher, P.; Bare, S. R. Limits of detection for EXAFS characterization of heterogeneous single-atom catalysts. *ACS. Catal.* **2023**, *13*, 6462-73. DOI
84. Chang, B.; Zhang, L.; Wu, S.; Sun, Z.; Cheng, Z. Engineering single-atom catalysts toward biomedical applications. *Chem. Soc. Rev.* **2022**, *51*, 3688-734. DOI
85. Li, L.; Wang, P.; Shao, Q.; Huang, X. Metallic nanostructures with low dimensionality for electrochemical water splitting. *Chem. Soc. Rev.* **2020**, *49*, 3072-106. DOI
86. Ning, Y.; Sun, Y.; Yang, X.; et al. Defect-rich CoFe-layered double hydroxides as superior peroxidase-like nanozymes for the detection of ascorbic acid. *ACS. Appl. Mater. Interfaces.* **2023**, *15*, 26263-72. DOI
87. Zheng, X.; Li, P.; Dou, S.; et al. Non-carbon-supported single-atom site catalysts for electrocatalysis. *Energy. Environ. Sci.* **2021**, *14*, 2809-58. DOI
88. Yu, Z.; Sun, Q.; Zhang, L.; et al. Research progress of amorphous catalysts in the field of electrocatalysis. *Microstructures* **2024**, *4*, 2024022. DOI
89. Mao, J.; Wang, Y.; Zhang, B.; et al. Advances in electrocarboxylation reactions with CO_2. *Green. Carbon.* **2024**, *2*, 45-56. DOI
90. Zeng, K.; Chao, M.; Tian, M.; et al. Atomically dispersed cerium sites immobilized on vanadium vacancies of monolayer nickel□vanadium layered double hydroxide: accelerating water splitting kinetics. *Adv. Funct. Mater.* **2024**, *34*, 2308533. DOI
91. Wang, B.; Han, X.; Guo, C.; et al. Structure inheritance strategy from MOF to edge-enriched NiFe-LDH array for enhanced oxygen evolution reaction. *Appl. Catal. B:. Environ.* **2021**, *298*, 120580. DOI
92. Wang, X.; Zhou, J.; Cui, W.; et al. Electron manipulation and surface reconstruction of bimetallic iron-nickel phosphide nanotubes for enhanced alkaline water electrolysis. *Adv. Sci.* **2024**, *11*, e2401207. DOI
93. Zhao, D.; Zhuang, Z.; Cao, X.; et al. Atomic site electrocatalysts for water splitting, oxygen reduction and selective oxidation. *Chem. Soc. Rev.* **2020**, *49*, 2215-64. DOI
94. Hameed, A.; Batool, M.; Liu, Z.; Nadeem, M. A.; Jin, R. Layered double hydroxide-derived nanomaterials for efficient electrocatalytic water splitting: recent progress and future perspective. *ACS. Energy. Lett.* **2022**, *7*, 3311-28. DOI
95. Zhang, J.; Liu, J.; Xi, L.; et al. Single-atom Au/NiFe layered double hydroxide electrocatalyst: probing the origin of activity for oxygen evolution reaction. *J. Am. Chem. Soc.* **2018**, *140*, 3876-9. DOI
96. Chen, X.; Wan, J.; Zheng, M.; et al. Engineering single atomic ruthenium on defective nickel vanadium layered double hydroxide for highly efficient hydrogen evolution. *Nano. Res.* **2023**, *16*, 4612-9. DOI
97. Biswal, S.; Divya; Mishra, B.; et al. Electronic modulation of iridium single atomic sites on NiCr layered double hydroxide for an

improved electrocatalytic oxygen evolution reaction. *J. Mater. Chem. A.* **2024**, *12*, 2491-500. DOI

98. Zeng, K.; Tian, M.; Chen, X.; et al. Strong electronic coupling between single Ru atoms and cobalt-vanadium layered double hydroxide harness efficient water splitting. *Chem. Eng. J.* **2023**, *452*, 139151. DOI
99. Yu, Z.; Liu, L. Recent Advances in hybrid seawater electrolysis for hydrogen production. *Adv. Mater.* **2024**, *36*, e2308647. DOI
100. Du, J.; Xiang, D.; Zhou, K.; et al. Electrochemical hydrogen production coupled with oxygen evolution, organic synthesis, and waste reforming. *Nano. Energy.* **2022**, *104*, 107875. DOI
101. Xu, H.; Xin, G.; Hu, W.; et al. Single-atoms Ru/NiFe layered double hydroxide electrocatalyst: efficient for oxidation of selective oxidation of 5-hydroxymethylfurfural and oxygen evolution reaction. *Appl. Catal. B:. Environ.* **2023**, *339*, 123157. DOI
102. Sun, H.; Li, L.; Chen, H. C.; et al. Highly efficient overall urea electrolysis via single-atomically active centers on layered double hydroxide. *Sci. Bull.* **2022**, *67*, 1763-75. DOI
103. Khalafallah, D.; Farghaly, A. A.; Ouyang, C.; Huang, W.; Hong, Z. Atomically dispersed Pt single sites and nanoengineered structural defects enable a high electrocatalytic activity and durability for hydrogen evolution reaction and overall urea electrolysis. *J. Power. Sources.* **2023**, *558*, 232563. DOI
104. Meng, G.; Chang, Z.; Zhu, L.; et al. Adsorption site regulations of [W-O]-doped CoP boosting the hydrazine oxidation-coupled hydrogen evolution at elevated current density. *Nano-Micro. Lett.* **2023**, *15*, 212. DOI
105. Wang, Z.; Xu, S. M.; Xu, Y.; et al. Single Ru atoms with precise coordination on a monolayer layered double hydroxide for efficient electrooxidation catalysis. *Chem. Sci.* **2019**, *10*, 378-84. DOI PubMed PMC
106. Li, L.; Zhang, N. Atomic dispersion of bulk/nano metals to atomic-sites catalysts and their application in thermal catalysis. *Nano. Res.* **2023**, *16*, 6380-401. DOI
107. Mori, K.; Taga, T.; Yamashita, H. Isolated single-atomic Ru catalyst bound on a layered double hydroxide for hydrogenation of CO_2 to formic acid. *ACS. Catal.* **2017**, *7*, 3147-51. DOI
108. Zhou, X.; Yang, Z.; Chen, Y.; et al. Single-atom Ru loaded on layered double hydroxide catalyzes peroxymonosulfate for effective E. *coli440*, 129720. DOI